Research Article

Extracting Maximum Information from Polarised Baryon Decays via Amplitude Analysis: The $\Lambda_c^+ \longrightarrow pK^-\pi^+$ Case

Daniele Marangotto [ORCID]

Università degli Studi di Milano and INFN Milano, Via Celoria 16, 20133 Milano, Italy

Correspondence should be addressed to Daniele Marangotto; daniele.marangotto@unimi.it

We consider what is the maximum information measurable from the decay distributions of polarised baryon decays via amplitude analysis in the helicity formalism. We focus in particular on the analytical study of the $\Lambda_c^+ \longrightarrow pK^-\pi^+$ decay distributions, demonstrating that the full information on its decay amplitudes can be extracted from its distributions, allowing a simultaneous measurement of both helicity amplitudes and the polarisation vector. This opens the possibility to use the $\Lambda_c^+ \longrightarrow pK^-\pi^+$ decay for applications ranging from New Physics searches to low-energy QCD studies, in particular its use as absolute polarimeter for the Λ_c^+ baryon. This result is valid as well for baryon decays having the same spin structure, and it is cross-checked numerically by means of a toy amplitude fit with Monte Carlo pseudodata.

1. Introduction

The study of the complete phase space distributions (i.e., the fully differential decay rate) of particle decays via angular or amplitude analysis allows to extract the maximum information about the process, since no integration is performed on the decay degrees of freedom. However, what is this maximum information for a given decay structure? Which parameters describing the phase space distributions can be measured? Indeed, in general, it is not guaranteed that the different functional forms characterising the decay distributions, separable by means of an amplitude fit, yield enough constraints on the parameters describing the decay in a given phenomenological framework. In this article, we study the constraints placed by the phase space distributions of baryon decays described in the helicity formalism, showing what information can be obtained under which conditions.

In particular, we focus on the $\Lambda_c^+ \longrightarrow pK^-\pi^+$ decay, whose amplitude analysis is ongoing at the LHCb experiment [1], demonstrating the possibility to extract the full information on its parameters, measuring both helicity amplitudes and the polarisation vector simultaneously, in the presence of nonnegligible polarisation. Thus, the $\Lambda_c^+ \longrightarrow pK^-\pi^+$ decay parameters can be considered as physical observables. This result is valid as well for polarised baryon decays having the same spin structure, a first parity-violating decay, and a subsequent parity-conserving decay. Since the present article is intended to be a phenomenological study, we will not consider experimental effects: we assume a sufficiently large fit statistics, allowing to effectively separate each phase space dependency, and an adequate description of the invariant mass lineshape functions which parametrise resonant contributions.

The possibility to extract the whole decay amplitude is a remarkable result given the strong interest in the measurement of the associated observables, ranging from New Physics searches to low-energy QCD studies. The full knowledge of the helicity amplitudes characterises each resonant contribution to the decay, both its squared modulus and phase, as well as the resonance polarisation. The comparison between observables measured for *CP* conjugated decays enables *CP* symmetry violation studies for specific contributions or localised in the phase space. Moreover, the knowledge of a particle decay amplitude allows to add information on its

production processes; for instance, the inclusion of the $\Lambda_c^+ \longrightarrow pK^-\pi^+$ amplitude model in $\Lambda_b^0 \longrightarrow \Lambda_c^+ l^- \bar{\nu}_l$ angular analyses increases the sensitivity to possible beyond the Standard Model physics contributions [2–9].

Considering baryon polarisation, the measurement of its absolute value and direction is essential for a variety of studies. Polarisation measurements for different production mechanisms give precious information on the baryon spin structure and formation process; for heavy baryons, they are expected to be closely related to the charm quark polarisation and its originating process [10]. Since the baryon polarisation is difficult to predict in QCD, being related to its nonperturbative regime, such measurements are useful to discriminate among different low energy QCD models.

Focusing on the Λ_c^+ baryon, its main decay channel $\Lambda_c^+ \longrightarrow pK^-\pi^+$ allows the measurement of its polarisation with the best statistical precision. Indeed, the two-body decay $\Lambda_c^+ \longrightarrow \Lambda\pi^+$, which can be used for polarisation measurements since its decay asymmetry parameter is known [11], has a lower branching fraction by a factor ≈ 5 [11] and reduced detector reconstruction efficiency because of the large Λ baryon flight distance, especially for fixed-target experiments. Moreover, the use of single resonant components of the $\Lambda_c^+ \longrightarrow pK^-\pi^+$ decay is not feasible because of its complicated decay structure characterised by many overlapping and interfering resonant contributions, making single components hardly to isolate [1].

A method to extract the Λ_c^+ polarisation with the best precision is fundamental for the proposed search of charm baryon electromagnetic dipole moments using bent crystals at the LHC [12], since dipole moments are to be inferred from spin precession.

A measurement of the Λ_c^+ polarisation in the $\Lambda_c^+ \longrightarrow pK^-\pi^+$ decay mode via amplitude analysis has already been performed by the E791 experiment [13]; however, the results obtained are not reliable: first, because a wrong amplitude model was employed, since no matching of proton spin states among different decay chains was performed; second, because no analytical or numerical study showed where the sensitivity to the polarisation came from. This study addresses for the first time the question for $\Lambda_c^+ \longrightarrow pK^-\pi^+$ decays. The decay distribution of different nonleptonic Λ_c^+ decays has been studied theoretically [14–16], also in connection with weak $\Lambda_b^0 \longrightarrow \Lambda_c^+$ transitions [17–19]. A precise determination of the $\Lambda_c^+ \longrightarrow pK^-\pi^+$ amplitude model would allow to test some theoretical predictions, for instance, the parity-conserving nature of the $\Lambda_c \longrightarrow \Delta^{++}K^-$ decay [14]. The Λ_c^+ longitudinal polarisation has been theoretically explored under $SU(3)$ flavor symmetry in Ref. [20].

We first introduce the formalism employed for the general expression of polarised decay rates in the helicity formalism, Section 2. We review the decay distributions of two-body and three-body via a single intermediate state baryon decays in Sections 3 and 4, respectively, stressing the role of the baryon polarisation in the determination of the decay rate. In the latter case, we consider the decay distributions associated to the spin structure $1/2 \longrightarrow S_R (\longrightarrow 1/2, 0), 0$, which is relevant, e.g., for $\Lambda_c^+ \longrightarrow \Lambda(\longrightarrow p\pi^-)\pi^+$ decays.

The core of the article is the study of the decay rate of three-body decays via multiple intermediate states, for the $\Lambda_c^+ \longrightarrow pK^-\pi^+$ case, Section 5. We show how the presence of significant interference effects together with a nonnegligible Λ_c^+ polarisation allows the simultaneous measurement of all the parameters characterising the $\Lambda_c^+ \longrightarrow pK^-\pi^+$ amplitude model, including complex helicity couplings and the polarisation vector. In Section 6, we cross-check the analytical study of the $\Lambda_c^+ \longrightarrow pK^-\pi^+$ decay rate by means of a toy amplitude fit on Monte Carlo generated pseudodata. The conclusions of the article are summarized in Section 7.

2. Formalism

2.1. Polarised Differential Decay Rate. We consider the differential decay rate for polarised particles, see, e.g., Ref. [21] for a more complete treatment of the subject. The generic spin state of a statistical ensemble of particles is described by means of a density operator: given an ensemble of spin states $|\psi\rangle_i$ occurring with probability p_i, the density operator is

$$\widehat{\rho} = \sum_i p_i |\psi\rangle_i \langle\psi|_i, \tag{1}$$

and the expectation value of any operator $\widehat{X}$ on the state described by $\widehat{p}$ can be expressed as

$$\langle\widehat{X}\rangle = \sum_i p_i \langle\psi|\widehat{X}|\psi\rangle_i = \mathrm{Tr}\left[\widehat{\rho}\widehat{X}\right]. \tag{2}$$

The decay rate of a multibody decay $A \longrightarrow \{i = 1, .., n\}$ for definite spin eigenstates is the squared modulus of the transition amplitude between the A particle initial state $|s_A, m_A\rangle$ and the final particle product state $|\{s_i\}, \{m_i\}\rangle = \otimes_i |s_i, m_i\rangle$,

$$p_{m_A, \{m_i\}}(\Omega) = \left|\langle s_A, m_A|\widehat{T}|\{s_i\}, \{m_i\}\rangle\right|^2$$
$$= \left|\mathscr{A}_{m_A, \{m_i\}}(\Omega)\right|^2. \tag{3}$$

The label Ω denotes the set of phase space variables describing the decay distributions.

Generic polarisation states are described by introducing the density operators for the initial particle state $\widehat{\rho}^A$ and the final particle state $\widehat{\rho}^{A\{i\}}$, which are included in the decay rate Eq. (3) by inserting suitable identity resolutions,

$$p\left(\Omega, \widehat{p}^A, \widehat{p}^{\{i\}}\right) = \mathrm{tr}\left[\widehat{p}^A, \widehat{p}^{\{i\}}\widehat{T}^\dagger\right] = \sum_{m_A, m_A'\{m_i\}, \{m_i'\}}$$
$$\cdot \widehat{p}^A_{m_A, m_A'}\widehat{p}^{\{i\}}_{\{m_i\}, \{m_i'\}}\mathscr{A}_{\{m_A\}\{m_i'\}} \tag{4}$$
$$\cdot (\Omega)\mathscr{A}^*_{\{m_A'\}\{m_i'\}}(\Omega).$$

The differential decay rate of a spin 1/2 particle in a generic polarisation state is derived considering its density matrix

$$\rho^A = \frac{1}{2}\left(\mathbb{I} + P \cdot \sigma\right) = \frac{1}{2}\left\{\begin{array}{cc} 1 + P_z & P_x - iP_y \\ P_x - iP_y & 1 - P_z \end{array}\right\}, \qquad (5)$$

in which the polarisation components P_x, P_y, P_z are the expectation values of the three spin operators and σ the three Pauli matrices. The final particle polarisation states, assumed to be unmeasurable, are described by an identity density matrix

$$\rho^{\{i\}} = \frac{\mathbb{I}}{2}. \qquad (6)$$

The differential rate Eq. (4), decomposed into unpolarised, longitudinal (P_z) and orthogonal (P_x, P_y) polarisation parts becomes

$$p(\Omega, P) = p_{unpol}(\Omega) + p_{long}(\Omega, P_z) + p_{orth}(\Omega, P_x, P_y), \qquad (7)$$

$$p_{unpol}(\Omega) = \frac{1}{2}\sum_{\{m_i\}}\left(\left|\mathscr{A}_{1/2,\{m_i\}}(\Omega)\right|^2 + \left|\mathscr{A}_{-1/2,\{m_i\}}(\Omega)\right|^2\right), \qquad (8)$$

$$p_{long}(\Omega, P_z) = \frac{1}{2}P_z\sum_{\{m_i\}}\left(\left|\mathscr{A}_{1/2,\{m_i\}}(\Omega)\right|^2 - \left|\mathscr{A}_{-1/2,\{m_i\}}(\Omega)\right|^2\right), \qquad (9)$$

$$p_{orth}(\Omega, P_x, P_y) = \text{Re}\left[\left(P_x - iP_y\right)\sum_{\{m_i\}}\mathscr{A}_{1/2,\{m_i\}}(\Omega)\mathscr{A}^*_{-1/2,\{m_i\}}(\Omega)\right]. \qquad (10)$$

2.2. General Properties of the Polarised Decay Rate.

For later convenience, we consider some properties of the polarised decay rate related to rotational invariance and parity symmetry.

The polarisation vector P associated to a decaying particle A is the only quantity specifying a direction in its rest frame. Therefore, rotational invariance implies that for null polarisation, the decay rate must be isotropic in any A rest frame defined independently from the decay distributions. In other words, the decay rate specifies the relative angular distribution among daughter particles, but not their global orientation in space.

For nonzero polarisation, both the polarisation vector and the daughter particle momenta transform in the same way under rotations. Thus, the relative orientation of daughter particles is independent on the polarisation vector.

The sensitivity of the decay rate to the particle polarisation depends critically on the amount of parity symmetry violation characterising the decay. Parity symmetry requires the decay angular distribution to be equal for $+|P|$ and $-|P|$ polarisation values, for any polarisation vector P, since parity transformation reverses the daughter particle momenta but not the polarisation vector. Therefore, a decay mediated by a parity conserving interaction retains no information on the decaying particle polarisation. Vice versa, the sensitivity of the decay rate on parity-violating effects depends critically on the amount of decaying particle polarisation. Indeed, since for zero polarisation, there is no preferred direction, the decay rate becomes symmetric under parity transformation, and parity-violating effects cancel.

One can see the combined effect of parity-violation and polarisation as creating an anisotropy along the direction specified by P. Rotational invariance makes all such directions equivalent, in the sense that a rotation of the system can only change the direction of the anisotropy. Indeed, given a generic polarisation, we can choose the z quantisation axis to be along P when studying the properties of the decay rate other than the polarisation direction. This is why in this article the sensitivity of the decay rate to its parameters like helicity couplings and polarisation modulus is usually studied assuming longitudinal polarisation only. Vice versa, the anisotropy can be used to determine the polarisation direction from the decay distributions, as will be shown in Section 3.

Note that, at the level of the observed decay distribution, parity-violation effects originated in the decay process may be in influenced by final state interactions. A theoretical study would be needed to disentangle the two contributions from the results of an amplitude fit.

2.3. Helicity Formalism.

We briefly introduce the helicity formalism following the method of Ref. [22], in which the helicity formalism is revisited in light of its application to multibody polarised particle decays, like the $\Lambda_c^+ \longrightarrow pK^-\pi^+$ one. The "standard" helicity formalism of Ref. [23, 24] is slightly modified to ease a correct matching of final particles spin states for decays featuring different interfering decay chains. For the case of two-body and three-body via a single intermediate state decays, Sections 3 and 4, where single decay amplitudes are involved, the two approaches coincide.

Two-body $A \longrightarrow 1, 2$ decay amplitudes can be expressed in terms of A spin state $|s_A, m_A\rangle$, and a 1,2 two-particle state being the product of particle 1 helicity states $|s_1, \lambda_1\rangle$ and particle 2 opposite-helicity states $|s_2, \bar{\lambda}_2\rangle$, as

$$\mathscr{A}_{m_A, \lambda_1, \bar{\lambda}_2}(\theta_1, \phi_1) = \langle \theta_1, \phi_1, \lambda_1, \bar{\lambda}_2 | \hat{T} | s_A, m_A \rangle = \mathscr{H}_{\lambda_1, \bar{\lambda}_2} D^{*s_A}_{m_A, \lambda_1 + \bar{\lambda}_2}(\phi_1, \theta_1, 0), \qquad (11)$$

in which θ_1, ϕ_1 are the spherical angles of the particle 1 momentum in the A reference system and D is a Wigner D matrix representing rotations on spin states (see, e.g., Ref. [25] for their definition and properties). The use of opposite-helicity states eases the control of phases arising from the helicity rotations. The complex number

$$\mathscr{H}_{\lambda_1, \bar{\lambda}_2} \equiv \langle s_A, m_A, \lambda_1, \bar{\lambda}_2 | \hat{T} | s_A, m_A \rangle, \qquad (12)$$

called helicity coupling, encodes the decay dynamics, and cannot depend on m_A for rotational invariance. The helicity values allowed by angular momentum conservation are

$$|\lambda_1| \le s_1, \tag{13}$$

$$|\bar{\lambda}_2| \le s_2, \tag{14}$$

$$|\lambda_1 + \bar{\lambda}_2| \le s_A. \tag{15}$$

Multibody decay amplitudes are treated in the helicity formalism by breaking the decay into sequences of two-body decays introducing suitable intermediate states and summing over their helicity states allowed by Eq. (13).

3. Two-Body Decay

We consider a two-body decay $A \longrightarrow 1, 2$ of a spin 1/2 particle in the helicity formalism introduced in Section 2.3. Following Eqs. (8) and (9), the longitudinal polarisation decay rate is

$$p(\theta_1, P_z) = \sum_{\lambda_1, \bar{\lambda}_2} \left|\mathscr{H}_{\lambda_1, \bar{\lambda}_2}\right|^2 \left(\frac{1 + P_z}{2} d^{1/2}_{1/2, \lambda_1 + \bar{\lambda}_2}(\theta_1)^2 \right. $$
$$\left. + \frac{1 - P_z}{2} d^{1/2}_{-1/2, \lambda_1 + \bar{\lambda}_2}(\theta_1)^2 \right), \tag{16}$$

with θ_1, ϕ_1 are the spherical angles of the particle 1 momentum in the A reference system. The rate cannot depend on the azimuthal angle ϕ_1 for invariance under rotations around the z-axis. Using the d-matrix property

$$\sum_m d^S_{m,m'}(\theta)^2 = 1, \tag{17}$$

and fixing the overall helicity coupling normalisation to

$$\sum_{\lambda_1, \bar{\lambda}_2} \left|\mathscr{H}_{\lambda_1, \bar{\lambda}_2}\right|^2 \equiv 1, \tag{18}$$

we find that for zero polarisation, the decay rate is constant, isotropic as required by rotational invariance. For nonzero polarisation, the decay rate takes the well-known form

$$p(\theta_1, P_z) = \frac{1}{2} + \frac{P_z}{2} \sum_{\lambda_1, \bar{\lambda}_2} \left|\mathscr{H}_{\lambda_1, \bar{\lambda}_2}\right|^2$$
$$\cdot \left(d^{1/2}_{1/2, \lambda_1 + \bar{\lambda}_2}(\theta_1)^2 - d^{1/2}_{-1/2, \lambda_1 + \bar{\lambda}_2}(\theta_1)^2 \right)$$
$$= \frac{1}{2} + \frac{P_z}{2} \cos\theta_1 \sum_{\lambda_1, \bar{\lambda}_2} \text{sign}(\lambda_1 + \bar{\lambda}_2) \left|\mathscr{H}_{\lambda_1, \bar{\lambda}_2}\right|^2$$
$$= \frac{1}{2} (1 + \alpha P_z \cos\theta_1), \tag{19}$$

in which the explicit expression for the d-matrices Eq. (A.1) has been used, and the decay asymmetry parameter

$$\alpha \equiv \sum_{\lambda_1, \bar{\lambda}_2} \text{sign}(\lambda_1 + \bar{\lambda}_2) \left|\mathscr{H}_{\lambda_1, \bar{\lambda}_2}\right|^2, \tag{20}$$

is introduced. The sensitivity to the polarisation is governed by the α parity-violating parameter. Indeed, α is zero if the decay conserves parity, which requires

$$\left|\mathscr{H}_{\lambda_1, \bar{\lambda}_2}\right|^2 = \left|\mathscr{H}_{-\lambda_1, -\bar{\lambda}_2}\right|^2. \tag{21}$$

Note that a fit to the $\cos\theta_1$ decay distribution can only measure the combination αP_z: it is not possible to determine separately the polarisation and the α parameter values, unless one of the two is available from other measurements. Moreover, the fit is not sensitive to the single helicity couplings, but only to the α combination.

For a generic A polarisation vector, the decay rate is, following Eqs. (8)–(10),

$$p(\theta_1, \phi_1, \boldsymbol{P}) = \frac{1}{2} \sum_{\lambda_1, \bar{\lambda}_2} \left|\mathscr{H}_{\lambda_1, \bar{\lambda}_2}\right|^2 \left[(1 + P_z) d^{1/2}_{1/2, \lambda_1 + \bar{\lambda}_2}(\theta_1)^2 \right.$$
$$+ (1 - P_z) d^{1/2}_{-1/2, \lambda_1 + \bar{\lambda}_2}(\theta_1)^2$$
$$+ 2(P_x \cos\phi_1 + P_y \sin\phi_1) d^{1/2}_{1/2, \lambda_1 + \bar{\lambda}_2}$$
$$\left. \cdot (\theta_1) d^{1/2}_{-1/2, \lambda_1 + \bar{\lambda}_2}(\theta_1) \right]. \tag{22}$$

The orthogonal polarisation part becomes

$$p_{\text{orth}}(\theta_1, \phi_1, P_x, P_y) = \sum_{\lambda_1, \bar{\lambda}_2} \text{sign}(\lambda_1 + \bar{\lambda}_2) \left|\mathscr{H}_{\lambda_1, \bar{\lambda}_2}\right|^2$$
$$\cdot (P_x \cos\phi_1 + P_y \sin\phi_1) \cos\frac{\theta_1}{2} \sin\frac{\theta_1}{2}$$
$$= \frac{1}{2}\alpha(P_x \cos\phi_1 + P_y \sin\phi_1) \sin\theta_1, \tag{23}$$

so that the decay rate is

$$p(\theta_1, \phi_1, \boldsymbol{P}) = \frac{1}{2} (1 + \alpha P_z \cos\theta_1 + \alpha P_x \sin\theta_1 \cos\phi_1$$
$$+ \alpha P_y \sin\theta_1 \sin\phi_1) = \frac{1}{2} (1 + \alpha \boldsymbol{P} \cdot \hat{\boldsymbol{p}}_1), \tag{24}$$

with $\hat{\boldsymbol{p}}_1$ being the particle 1 momentum versor in the A reference system. It features three angular distributions, each describing a different polarisation component, all multiplied by the α parameter. Therefore, a fit can determine the polarisation direction, but not its modulus independently of α. Note that the orthogonal polarisation part does not add information on the helicity couplings, which enter the decay rate only via the α combination.

4. Three-Body Decay via a Single Intermediate State

We consider a three-body decay with a single intermediate state R of the form $A \longrightarrow R(\longrightarrow 1, 2), 3$, with spin structure $1/2 \longrightarrow S_R(\longrightarrow 1/2, 0), 0$. Summing over the resonance helicity states allowed by angular momentum conservation, the decay amplitude is

$$
\mathcal{A}_{m_A, \lambda_1} = \sum_{\lambda_R = \pm 1/2} \mathcal{H}^A_{\lambda_R, 0} D^{*1/2}_{m_A, \lambda_R}(\phi_R, \theta_R, 0) \mathcal{H}^R_{\lambda_1, 0} D^{*S_R}_{\lambda_R, \lambda_1} \\
\cdot (\phi_1, \theta_1, 0) \mathcal{R}_R(m_R^2),
\tag{25}
$$

in which θ_R, ϕ_R are the spherical angles of the R momentum in the A reference system, θ_1, ϕ_1 now are the spherical angles of the particle 1 momentum in the R helicity reference system, λ_R is the R helicity defined from the A system, and λ_1 is the particle 1 helicity defined from the R helicity system. The helicity couplings $\mathcal{H}^A_{\lambda_R, 0}$ and $\mathcal{H}^A_{\lambda_1, 0}$ are associated to the two-body decays $A \longrightarrow R, 3$ and $R \longrightarrow 1, 2$, respectively. A nonnegligible width for the R state has been assumed, its invariant mass dependence described by the lineshape function $\mathcal{R}_R(m_R^2)$. The squared modulus is

$$
\begin{aligned}
\left| \mathcal{A}_{m_a, \lambda_1} \right|^2 = & \left[\left| \mathcal{H}^A_{1/2, 0} \right|^2 \left| \mathcal{H}^R_{\lambda_1, 0} \right|^2 d^{1/2}_{m_A, 1/2}(\theta_R)^2 d^{S_R}_{1/2, \lambda_1}(\theta_1)^2 \right. \\
& + \left| \mathcal{H}^A_{-1/2, 0} \right|^2 \left| \mathcal{H}^R_{\lambda_1, 0} \right|^2 d^{1/2}_{m_A, -1/2}(\theta_R)^2 d^{S_R}_{-1/2, \lambda_1}(\theta_1)^2 \\
& + 2 \operatorname{Re} \left(\mathcal{H}^A_{1/2, 0} \mathcal{H}^{*A}_{-1/2, 0} e^{i\phi_1} \right) d^{1/2}_{m_A, 1/2}(\theta_R) d^{1/2}_{m_A, -1/2}(\theta_R) \\
& \left. \cdot \left| \mathcal{H}^R_{\lambda_1, 0} \right|^2 d^{S_R}_{1/2, \lambda_1}(\theta_1) d^{S_R}_{-1/2, \lambda_1}(\theta_1) \right] \times \left| \mathcal{R}_R(m_R^2) \right|^2.
\end{aligned}
\tag{26}
$$

Let us consider the unpolarised decay rate Eq. (8): using

$$
\sum_{m_A = \pm 1/2} d^{1/2}_{m_A, \lambda}(\theta_R)^2 = 1, \quad \sum_{m_A = \pm 1/2} d^{1/2}_{m_A, 1/2}(\theta_R) d^{1/2}_{m_A, -1/2}(\theta_R) = 0,
\tag{27}
$$

and the explicit d-matrix element values Eqs. (A.1) and (A.2), we find

$$
\begin{aligned}
p_{\text{unpol}}(m_R^2, \theta_1) = & \frac{1}{2} \left(\left| \mathcal{H}^A_{1/2, 0} \right|^2 \left| \mathcal{H}^R_{1/2, 0} \right|^2 + \left| \mathcal{H}^A_{-1/2, 0} \right|^2 \left| \mathcal{H}^R_{-1/2, 0} \right|^2 \right) \\
& \cdot \left| g^{S_R}_R(m_R^2, \theta_1) \right|^2 \cos^2 \frac{\theta_1}{2} + \frac{1}{2} \left(\left| \mathcal{H}^A_{1/2, 0} \right|^2 \right. \\
& \cdot \left| \mathcal{H}^R_{-1/2, 0} \right|^2 + \left| \mathcal{H}^A_{-1/2, 0} \right|^2 \left| \mathcal{H}^R_{1/2, 0} \right|^2 \right) \\
& \cdot \left| g^{S_R}_R(m_R^2, \theta_1) \right|^2 \sin^2 \frac{\theta_1}{2},
\end{aligned}
\tag{28}
$$

in which

$$
g^{S_R}_R(m_R^2, \theta_1) \equiv f(S_R, \theta_1) \mathcal{R}_R(m_R^2),
\tag{29}
$$

with $f(S_R, \theta_1)$ describing the angular distribution of the state R for $S_R > 1/2$, see Appendix A. The rate can be arranged in the form (playing with the $\cos^2 \alpha + \sin^2 \alpha = 1$ relation)

$$
p_{\text{unpol}}(m_R^2, \theta_1) = \frac{1}{4}(1 + \alpha_A \alpha_R \cos \theta_1) \left| g^{S_R}_R(m_R^2, \theta_1) \right|^2,
\tag{30}
$$

by using the normalisation condition Eq. (18) and the definition of the asymmetry parameters for the two-body decays $A \longrightarrow R, 3$ and $R \longrightarrow 1, 2$,

$$
\alpha_A \equiv \left| \mathcal{H}^A_{1/2, 0} \right|^2 - \left| \mathcal{H}^A_{-1/2, 0} \right|^2, \quad \alpha_R \equiv \left| \mathcal{H}^R_{1/2, 0} \right|^2 - \left| \mathcal{H}^R_{-1/2, 0} \right|^2.
\tag{31}
$$

A fit to the $\cos \theta_1$ distribution determines the combination $\alpha_A \alpha_R$, and the two cannot be separated unless one of the two is already measured. Note that the different form of the $\cos \theta_1$ distribution for different S_R values can be exploited to measure the R spin if not known.

The longitudinal polarisation decay rate Eqs. (8) and (9), applying

$$
d^{1/2}_{1/2, \lambda}(\theta_R)^2 - d^{1/2}_{-1/2, \lambda}(\theta_R)^2 = \cos^2 \frac{\theta_R}{2} - \sin^2 \frac{\theta_R}{2} = \cos \theta_R,
\tag{32}
$$

and

$$
\begin{aligned}
& d^{1/2}_{1/2, 1/2}(\theta_R) d^{1/2}_{1/2, -1/2}(\theta_R) - d^{1/2}_{-1/2, 1/2}(\theta_R) d^{1/2}_{-1/2, -1/2}(\theta_R) \\
& = -2 \cos \frac{\theta_R}{2} \sin \frac{\theta_R}{2} = -\sin \theta_R,
\end{aligned}
\tag{33}
$$

becomes equal to

$$
\begin{aligned}
& p(m_R^2, \theta_R, \theta_1, \phi_1, P_z) \\
& = p_{\text{unpol}}(\theta_1) + \frac{1}{2} P_z \cos \theta_R \\
& \quad \cdot \left(\left| \mathcal{H}^A_{1/2} \right|^2 \left| \mathcal{H}^R_{1/2} \right|^2 - \left| \mathcal{H}^A_{-1/2} \right|^2 \left| \mathcal{H}^R_{-1/2} \right|^2 \right) \\
& \quad \cdot \left| g^{S_R}_R(m_R^2, \theta_1) \right|^2 \cos^2 \frac{\theta_1}{2} + \frac{1}{2} P_z \cos \theta_R \\
& \quad \cdot \left(\left| \mathcal{H}^A_{1/2} \right|^2 \left| \mathcal{H}^R_{-1/2} \right|^2 - \left| \mathcal{H}^A_{-1/2} \right|^2 \left| \mathcal{H}^R_{1/2} \right|^2 \right) \\
& \quad \cdot \left| g^{S_R}_R(m_R^2, \theta_1) \right|^2 \sin^2 \frac{\theta_1}{2} + \frac{1}{2} P_z \operatorname{Re} \left(\mathcal{H}^A_{1/2} \mathcal{H}^{*A}_{-1/2} e^{i\phi_1} \right) \\
& \quad \cdot \left| \mathcal{H}^R_{1/2} \right|^2 (-\sin \theta_R) \left| g^{S_R}_R(m_R^2, \theta_1) \right|^2 \sin \theta_1 \\
& \quad + \frac{1}{2} P_z \operatorname{Re} \left(\mathcal{H}^A_{1/2} \mathcal{H}^{*A}_{-1/2} e^{i\phi_1} \right) \left| \mathcal{H}^R_{-1/2} \right|^2 (\sin \theta_R) \\
& \quad \cdot \left| g^{S_R}_R(m_R^2, \theta_1) \right|^2 \sin \theta_1.
\end{aligned}
\tag{34}
$$

In a similar way as before, the longitudinal polarisation decay rate can be written as

$$
\begin{aligned}
p\left(m_R^2, \theta_R, \theta_1, \phi_1, P_z\right) = {} & \frac{1}{4}\left(1 + \alpha_A \alpha_R \cos\theta_1\right)\left|g_R^{S_R}\left(m_R^2, \theta_1\right)\right|^2 \\
& + \frac{1}{4}P_z \cos\theta_R\left(\alpha_A + \alpha_R \cos\theta_1\right) \\
& \cdot \left|g_R^{S_R}\left(m_R^2, \theta_1\right)\right|^2 - \frac{1}{2}P_z\alpha_R \\
& \cdot \left|\mathscr{H}_{1/2}^A \mathscr{H}_{-1/2}^{*A}\right| \cos\left(\phi_1 \right. \\
& \left. + \Phi_A\right) \sin\theta_R \left|g_R^{S_R}\left(m_R^2, \theta_1\right)\right|^2 \sin\theta_1.
\end{aligned}
\tag{35}
$$

in which $\Phi_A = \arg \mathscr{H}_{1/2}^A \mathscr{H}_{-1/2}^{*A}$ is the relative phase between the two $A \longrightarrow R,3$ decay helicity couplings.

A fit to this decay distribution yields five constraints in total. The first two lines of Eq. (35) determine the three products $\alpha_A \alpha_R$, $P_z \alpha_A$, and $P_z \alpha_R$: it is possible to separately extract $\alpha_A \alpha_R$ and P_z if each one is different from zero. If the intermediate state decay conserves parity, $\alpha_R = 0$, the decay distribution becomes analogous to that of the two-body $A \longrightarrow R,3$ decay, Eq. (19),

$$
p\left(m_R^2, \theta_R, \theta_1, P_z\right) = \frac{1}{2}\left(1 + P_z \alpha_A \cos\theta_R\right)\left|g_R^{S_R}\left(m_R^2, \theta_1\right)\right|^2, \tag{36}
$$

for which P_z and α_A cannot be separately measured.

The last term of Eq. (35) allows the determination of $\left|\mathscr{H}_{1/2}^A \mathscr{H}_{-1/2}^{*A}\right|$ and Φ_A from the amplitude and phase of the ϕ_1 oscillation, provided both P_z and α_R are nonzero. Therefore, in the presence of a sizeable polarisation and of two subsequent parity-violating decays, the helicity couplings associated to the $A \longrightarrow R,3$ process are entirely measurable from the decay distributions, separately from the polarisation degree, since the decay rate gives 5 constraints on 5 real parameters (two for each complex coupling). In the following section, we will show how the same is valid for the $\Lambda_c^+ \longrightarrow pK^-\pi^+$ decay as well, but for one difference: here, one of the crucial conditions is parity-violation in the R decay; there, it is the interference among resonant contributions.

5. Three-Body Decay via Multiple Intermediate States: The $\Lambda_c^+ \longrightarrow pK^-\pi^+$ Case

In this section, we study baryon three-body decays via multiple interfering intermediate states, considering parity-violating baryon decays to intermediate states decaying via parity-conserving interactions. We take $\Lambda_c^+ \longrightarrow pK^-\pi^+$ decays as an explicit example, but the results obtained in this section hold for any three-body decay with spin structure 1/2 $\longrightarrow$ 1/2 0 0. The study of the $\Lambda_c^+ \longrightarrow pK^-\pi^+$ decay distributions is complicated because of the different interfering decay chains, and it is split into the following parts.

First, we introduce the description of the three-body phase space and the Dalitz plot decomposition [26], Section

5.1, which allows to separate invariant mass and decay orientation degrees of freedom in the decay amplitude. In Section 5.2, we perform a general study of the $\Lambda_c^+ \longrightarrow pK^-\pi^+$ polarised decay rate, while in Section 5.3, we write the complete $\Lambda_c^+ \longrightarrow pK^-\pi^+$ decay amplitude written in the helicity formalism following the method of Ref. [22]. The study of the $\Lambda_c^+ \longrightarrow pK^-\pi^+$ rate is developed in Section 5.4.

5.1. Three-Body Decay Phase Space and Dalitz Plot Decomposition. A particle three-body decay is described by 5 degrees of freedom, resulting from 12 four-momentum components constrained by 3 mass requirements and 4 energy-momentum conservation relations, which confine the daughter's momenta to a plane in the rest frame of the mother particle. For unpolarised particles, the decay plane orientation is irrelevant, and the decay can be described by two two-body invariant masses (Dalitz variables). For the $\Lambda_c^+ \longrightarrow pK^-\pi^+$ decay, $m_{pK^-}^2$ and $m_{K^-\pi^+}^2$ are selected. For non-zero polarisation, the orientation of the decay plane must be specified with respect to the Λ_c^+ spin coordinate system. The orientation can be expressed by means of the three Euler angles (introduced, e.g., in Ref. [24]) describing the rotation from the Λ_c^+ spin coordinate system to a decay plane reference system, chosen in such a way that the proton momentum defines the z-axis, while the component of the kaon momentum orthogonal to the proton momentum defines the x-axis,

$$
\hat{\boldsymbol{z}}_{DP} = \hat{\boldsymbol{p}}(p), \quad \hat{\boldsymbol{x}}_{DP} = \frac{\boldsymbol{p}(p) \times \boldsymbol{p}(K^-)}{\left|\boldsymbol{p}(p) \times \boldsymbol{p}(K^-)\right|} \times \hat{\boldsymbol{p}}(p), \quad \hat{\boldsymbol{y}}_{DP} = \hat{\boldsymbol{z}}_{DP} \times \hat{\boldsymbol{x}}_{DP},
\tag{37}
$$

in which momenta are expressed in the Λ_c^+ rest frame. With this definition the α Euler angle is the azimuthal angle of the proton in the Λ_c^+ polarisation frame, ϕ_p, the β angle is the polar angle of the proton, θ_p, and the γ angle is the signed angle between the plane formed by the proton and the Λ_c^+ quantisation axis and the plane formed by the kaon and the pion, named χ.

The five variables describing a uniform phase space density can be chosen to be

$$
\Omega = \left(m_{pK^-}^2, m_{K^-\pi^+}^2, \cos\theta_p, \phi_p, \chi\right).
\tag{38}
$$

To simplify the $\Lambda_c^+ \longrightarrow pK^-\pi^+$ amplitude model expression, it is useful to separate invariant mass and decay orientation degrees of freedom applying the Dalitz plot decomposition proposed in Ref. [26]. Moreover, the properties following from rotational invariance described in Section 2.2 are enforced by construction. For the $\Lambda_c^+ \longrightarrow pK^-\pi^+$ decay, the decomposition is written as

$$
\mathscr{A}_{m_{\Lambda_c^+}, m_p}(\Omega) = \sum_{\nu_{\Lambda_c^+}} D_{m_{\Lambda_c^+}, \nu_{\Lambda_c^+}}^{*1/2}\left(\phi_p, \theta_p, \chi\right) \mathscr{O}_{\nu_{\Lambda_c^+}, m_p}\left(m_{pK^-}^2, m_{K^-\pi^+}^2\right),
\tag{39}
$$

in which the Wigner D-matrix describes the rotation of $|1/2, \mu_{\Lambda_c^+}\rangle$ Λ_c^+ spin states to those associated to the decay plane system Eq. (37), $|1/2, \nu_{\Lambda_c^+}\rangle$. The term $\mathcal{O}_{\nu_{\Lambda_c^+}, m_p}(m_{pK^-}^2, m_{K^-\pi^+}^2)$ is the decay amplitude in terms of $|1/2, \nu_{\Lambda_c^+}\rangle$ states and proton states defined in the canonical spin system reached from the Λ_c^+ decay plane system, $|1/2, m_p\rangle$. These proton states are needed for the matching of proton spin states among different decay chains.

5.2. General Study of the $\Lambda_c^+ \longrightarrow pK^-\pi^+$ Polarised Decay Rate. In the following, we present the general structure of the decay rate written applying the Dalitz plot decomposition for different polarisation characteristics. We consider the decay rate decomposed into unpolarised, longitudinal, and orthogonal polarisation parts Eqs. (8)–(10), with Eq. (39) applied to the decay amplitudes.

The unpolarised decay rate Eq. (8) is simply

$$p_{\text{unpol}}\left(m_{pK^-}^2, m_{K^-\pi^+}^2\right) = \sum_{\nu_{\Lambda_c^+}, m_p = \pm 1/2} \left|\mathcal{O}_{\nu_{\Lambda_c^+}, m_p}\right|^2, \qquad (40)$$

because of the orthogonality of Wigner D-matrices

$$\sum_m D_{m,\nu}^{*1/2}\left(\phi_p, \theta_p, \chi\right) D_{m,\nu'}^{1/2}\left(\phi_p, \theta_p, \chi\right) \propto \delta_{\nu,\nu'}, \qquad (41)$$

and does not depend on the orientation angles for rotational invariance.

The decay rate for longitudinal polarisation Eq. (9) can be written in the form

$$p_{\text{long}}(\Omega, P_z) = P_z\left[\cos\theta_p A\left(m_{pK^-}^2, m_{K^-\pi^+}^2\right) - 2\sin\theta_p \operatorname{Re} B\left(m_{pK^-}^2, m_{K^-\pi^+}^2, \chi\right)\right], \qquad (42)$$

with

$$A\left(m_{pK^-}^2, m_{K^-\pi^+}^2\right) \equiv \sum_{m_p}\left(\left|\mathcal{O}_{1/2, m_p}\right|^2 - \left|\mathcal{O}_{-1/2, m_p}\right|^2\right),$$

$$B\left(m_{pK^-}^2, m_{K^-\pi^+}^2, \chi\right) \equiv \sum_{m_p}\left(\exp i\chi\, \mathcal{O}_{1/2, m_p}\, \mathcal{O}_{-1/2, m_p}^*\right). \qquad (43)$$

The first term introduces a simple $\cos\theta_p$ linear dependence; the behaviour of the second term can be seen as follows. Let us write

$$\mathcal{O}_{1/2, m_p}\, \mathcal{O}_{-1/2, m_p}^* \equiv P_{m_p}\exp i\Phi_{m_p}, \qquad (44)$$

so that

$$\operatorname{Re} B\left(m_{pK^-}^2, m_{K^-\pi^+}^2, \chi\right) = \sum_{m_p} P_{m_p}\cos\left(\chi + \Phi_{m_p}\right)$$

$$\equiv P\cos\left(\chi + \Phi\right), \qquad (45)$$

is the sum of two cosine functions with different amplitude and phase but the same frequency in χ, which is equivalent to a single cosine function with some amplitude P and phase Φ. Since

$$\int_{-1}^{1}\sin\theta_p\, d\cos\theta_p = \frac{\pi}{2}, \qquad (46)$$

the oscillatory dependence of the Re B term is visible in the χ projection of the amplitude model. With projection, we refer to the one-dimensional decay distribution obtained integrating over all the phase space variables but one. Instead, the $\sin\theta_p$ dependence is not visible in the $\cos\theta_p$ projection since

$$\int_{-\pi}^{\pi} P\cos\left(\chi + \Phi\right)d\chi = 0. \qquad (47)$$

The decay rate for orthogonal polarisation can be written in the form

$$p_{\text{orth}}\left(\Omega, P_x, P_y\right) = \left(P_x\cos\phi_p - P_y\sin\phi_p\right)\left[\sin\theta_p A\left(m_{pK^-}^2, m_{K^-\pi^+}^2\right)\right.$$
$$+ 2\cos\theta_p \operatorname{Re} B\left(m_{pK^-}^2, m_{K^-\pi^+}^2, \chi\right)$$
$$\left. + 2i\operatorname{Im} B\left(m_{pK^-}^2, m_{K^-\pi^+}^2, \chi\right)\right], \qquad (48)$$

by exploiting the relation

$$a\cos^2\alpha - a^*\sin^2\alpha = \operatorname{Re} a\cos 2\alpha + i\operatorname{Im} a. \qquad (49)$$

For Eq. (46), the cosine (minus sine) dependence shows up in the ϕ_p projection, providing a clear signature for the presence of $P_x(P_y)$ orthogonal polarisation. Instead, orthogonal polarisation does not introduce effects in θ_p and χ projections, since

$$\int_{-\pi}^{\pi}\cos\phi_p d\phi_p = \int_{-\pi}^{\pi}\sin\phi_p d\phi_p = 0. \qquad (50)$$

The predicted dependence of the phase space variable projections on different Λ_c^+ polarisation components is shown with the use of Monte Carlo generated data for the toy amplitude model defined in Section 6 in Appendix B.

5.3. Decay Amplitudes in the Helicity Formalism. The $\Lambda_c^+ \longrightarrow pK^-\pi^+$ decay amplitudes $\mathcal{O}_{\nu_{\Lambda_c^+}, m_p}$ are written in the helicity formalism described in Section 2.3. We first consider the decay chain $\Lambda_c^+ \longrightarrow pK^*(\longrightarrow K^-\pi^+)$. The weak decay $\Lambda_c^+ \longrightarrow pK^*$ can be described by Eq. (11) applied starting from the decay plane coordinate system,

$$\mathcal{A}_{\nu_{\Lambda_c^+}, m_p, \bar{\lambda}_{K^*}}^{\Lambda_c^+ \to pK^*} = \mathcal{H}_{m_p, \bar{\lambda}_{K^*}}^{\Lambda_c^+ \to pK^*}\delta_{\nu_{\Lambda_c^+}, m_p + \bar{\lambda}_{K^*}}, \qquad (51)$$

so that the amplitude is written in terms of the proton spin m_p and the K^* opposite helicity $\bar{\lambda}_{K^*}$. Since no rotation of spin

states is involved, the D-matrix becomes a constraint on the helicity values $m_p + \bar{\lambda}_{K^*} = \nu_{\Lambda_c^+}$.

For spin zero K^* resonances, the angular momentum conservation relations Eq. (13) allow two complex couplings corresponding to $m_p = \pm 1/2$; for higher spin resonances, four couplings are allowed, corresponding to $\{m_p = 1/2, \bar{\lambda}_{K^*} = 0, -1\}$ and $\{m_p = -1/2, \bar{\lambda}_{K^*} = 0, 1\}$. The couplings are independent of each other because of parity violation in weak decays. The strong decay $K^* \longrightarrow K^- \pi^+$ contribution is

$$\mathscr{A}_{\bar{\lambda}_{K^*}}^{K^* \to K^- \pi^+} = \mathscr{H}_{0,0}^{K^* \to K^- \pi^+} d_{\bar{\lambda}_{K^*},0}^{*S_{K^*}}\left(\overline{\theta}_K\right) \mathscr{R}\left(m_{K^-\pi^+}^2\right), \quad (52)$$

in which $\mathscr{R}(m_{K^-\pi^+}^2)$ is the lineshape of the K^* resonance and $\overline{\theta}_K$ is the kaon momentum signed polar angle in the K^* opposite-helicity coordinate system,

$$\overline{\theta}_K = \text{atan2}\left(p_x^{K^*}(K^-), p_z^{K^*}(K^-)\right). \quad (53)$$

Signed polar angles are used as helicity angles in order to have rotations only around the y-axis of the decay plane system. Otherwise, the use of positive polar angles would require additional azimuthal rotations around the z-axis (to flip the y-axis direction) complicating unnecessarily the expression of the helicity amplitudes. In the fit model, the coupling $\mathscr{H}_{0,0}^{K^* \to K^- \pi^+}$ cannot be determined independently of $\mathscr{H}_{m_p, \bar{\lambda}_{K^*}}^{\Lambda_c^+ \to K^* p}$ couplings; therefore, it is set equal to 1 and absorbed into the latter.

Considering the decay chain $\Lambda_c^+ \longrightarrow \Lambda^*(\longrightarrow pK^-)\pi^+$, the weak decay $\Lambda_c^+ \longrightarrow \Lambda^* \pi^+$ is described by Eq. (11) as

$$\mathscr{A}_{\nu_{\Lambda_c^+},\lambda_{\Lambda^*}}^{\Lambda_c^+ \to \Lambda^* \pi^+} = \mathscr{H}_{\lambda_{\Lambda^*},0}^{\Lambda_c^+ \to \Lambda^* \pi^+} d_{\nu_{\Lambda_c^+},\lambda_{\Lambda^*}}^{1/2}(\theta_{\Lambda^*}), \quad (54)$$

in which λ_{Λ^*} is the Λ^* helicity system reached from the Λ_c^+ system and θ_{Λ^*} is the signed polar angle of the Λ^* momentum, defined as

$$\theta_{\Lambda^*} = \text{atan2}\left(p_x^{\Lambda_c^+}(\Lambda^*), p_z^{\Lambda_c^+}(\Lambda^*)\right). \quad (55)$$

The angular momentum conservation relations Eq. (13) allow two helicity couplings, $\lambda_{\Lambda^*} = \pm 1/2$, to fit for each resonance whatever S_{Λ^*} is. The strong decay $\Lambda^* \longrightarrow pK^-$ is described by

$$\mathscr{A}_{\lambda_{\Lambda^*},\lambda_p^{\Lambda^*}}^{\Lambda^* \to pK^-} = \mathscr{H}_{\lambda_p^{\Lambda^*},0}^{\Lambda^* \to pK^-} d_{\lambda_{\Lambda^*},\lambda_p^{\Lambda^*}}^{S_{\Lambda^*}}\left(\theta_p^{\Lambda^*}\right) \mathscr{R}\left(m_{pK^-}^2\right), \quad (56)$$

in which $\lambda_p^{\Lambda^*}$ is the proton helicity and $\theta_p^{\Lambda^*}$ is the proton signed polar angle in the helicity coordinate system reached from the Λ^* resonance. Since strong decays conserve parity, the two helicity couplings corresponding to $\lambda_p^{\Lambda^*} = \pm 1/2$ are related,

$$\mathscr{H}_{-\lambda_p^{\Lambda^*},0}^{\Lambda^* \to pK^-} = -P_{\Lambda^*}(-1)^{S_{\Lambda^*}-1/2} \mathscr{H}_{\lambda_p^{\Lambda^*},0}^{\Lambda^* \to pK^-}, \quad (57)$$

in which P_{Λ^*} is the parity of the Λ^* resonance and the proton and kaon parities $P_p = 1$, $P_K = -1$ have been inserted. In the fit model, these couplings are absorbed into $\mathscr{H}_{\lambda_{\Lambda^*},0}^{\Lambda_c^+ \to \Lambda^* \pi^+}$, setting $\mathscr{H}_{+1/2,0}^{\Lambda^* \to pK^-} = 1$ and $\mathscr{H}_{-1/2,0}^{\Lambda^* \to pK^-} = -P_{\Lambda^*}(-1)^{S_{\Lambda^*}-1/2}$.

The matching of proton spin states from the Λ^* helicity system to the canonical system is performed applying the method of Ref. [22] to the case of the Dalitz-plot decomposition. Indeed, the transformation sequence applied to reach the proton helicity frame must be undone step-by-step in order to ensure a consistent phase definition of fermion spin states. Three rotations must be applied to the proton spin system: two of angles $\theta_p^{\Lambda^*}$ and θ_{Λ^*}, plus the Wigner rotation accounting for the different boost sequence applied to reach the two systems. The Wigner rotation can be written in angle-axis decomposition [27], with angle

$$\alpha_{\Lambda^*}^W = \arccos\left[\frac{\left(1 + \gamma_p^{\Lambda_c^+} + \gamma_{\Lambda^*}^{\Lambda_c^+} + \gamma_p^{\Lambda^*}\right)^2}{\left(1 + \gamma_p^{\Lambda_c^+}\right)\left(1 + \gamma_{\Lambda^*}^{\Lambda_c^+}\right)\left(1 + \gamma_p^{\Lambda^*}\right)} - 1\right], \quad (58)$$

with γ_B^A the gamma factor of the boost connecting A and B systems, and axis

$$\boldsymbol{\alpha}_{\Lambda^*}^W = \frac{\boldsymbol{p}^{\Lambda_c^+}(\Lambda^*) \times \boldsymbol{p}^{\Lambda^*}(p)}{\left|\boldsymbol{p}^{\Lambda_c^+}(\Lambda^*) \times \boldsymbol{p}^{\Lambda^*}(p)\right|} = \widehat{\boldsymbol{y}}_{DP}, \quad (59)$$

i.e., the y-axis of the decay plane coordinate system. All these rotations are around the same y-axis, combined into one rotation $R_y(\beta_{\Lambda^*})$, with

$$\beta_{\Lambda^*} = \theta_p^{\Lambda^*} + \theta_{\Lambda^*} + \alpha_{\Lambda^*}^W. \quad (60)$$

Considering the third decay chain $\Lambda_c^+ \longrightarrow \Delta^{++*}(\longrightarrow p\pi^+)K^-$, the weak decay $\Lambda_c^+ \longrightarrow \Delta^{++*}K^-$ is described by

$$\mathscr{A}_{\nu_{\Lambda_c^+},\lambda_{\Delta^*}}^{\Lambda_c^+ \to \Delta^{++*}K^-} = \mathscr{H}_{\lambda_{\Delta^*},0}^{\Lambda_c^+ \to \Delta^{++*}K^-} d_{\nu_{\Lambda_c^+},\lambda_{\Delta^*}}^{1/2}(\theta_{\Delta^*}), \quad (61)$$

in which λ_{Δ^*} is the Δ^* helicity and θ_{Δ^*} is the signed polar angle of the Δ^* momentum in the Λ_c^+ rest frame with decay plane coordinate system. As for the Λ^* decay chain, there are two helicity couplings corresponding to $\lambda_{\Delta^*} = \pm 1/2$ to fit for each resonance. The strong decay $\Delta^{++*} \longrightarrow p\pi^+$ amplitude is written as

$$\mathscr{A}_{\lambda_{\Delta^*},\lambda_p^{\Delta^*}}^{\Delta^{++*} \to p\pi^+} = \mathscr{H}_{\lambda_p^{\Delta^*},0}^{\Delta^{++*} \to p\pi^+} d_{\lambda_{\Delta^*},\lambda_p^{\Delta^*}}^{S_{\Delta^*}}\left(\theta_p^{\Delta^*}\right) \mathscr{R}\left(m_{p\pi^+}^2\right), \quad (62)$$

in which $\lambda_p^{\Delta^*}$ is the proton helicity and $\theta_p^{\Delta^*}$ is the signed polar angle defined in the Λ^* helicity coordinate system. In the fit model, the strong decay helicity couplings are absorbed into $\mathscr{H}_{\lambda_{\Delta^*},0}^{\Lambda_c^+ \to \Delta^{++*}K^-}$ setting them to $\mathscr{H}_{+1/2,0}^{\Delta^{++*} \to p\pi^+} = 1$ and $\mathscr{H}_{-1/2,0}^{\Delta^{++*} \to p\pi^+} = -P_{\Delta^*}(-1)^{S_{\Delta^*}-1/2}$.

The matching of proton spin states from the Δ^* helicity system to the canonical system is performed similarly to the Λ^* decay chain. The Wigner rotation angle is

$$\alpha_{\Delta^*}^W = \arccos \left[\frac{\left(1 + \gamma_p^{\Lambda_c^+} + \gamma_{\Delta^*}^{\Lambda_c^+} + \gamma_p^{\Delta^*}\right)^2}{\left(1 + \gamma_p^{\Lambda_c^+}\right)\left(1 + \gamma_{\Delta^*}^{\Lambda_c^+}\right)\left(1 + \gamma_p^{\Delta^*}\right)} - 1 \right], \quad (63)$$

around the axis

$$\boldsymbol{\alpha}_{\Delta^*}^W = \frac{\boldsymbol{p}^{\Lambda_c^+}(\Delta^*) \times \boldsymbol{p}^{\Delta^*}(p)}{\left| \boldsymbol{p}^{\Lambda_c^+}(\Delta^*) \times \boldsymbol{p}^{\Delta^*}(p) \right|} = -\widehat{\boldsymbol{y}}_{DP}, \quad (64)$$

which is opposite to the y-axis of the decay plane coordinate system. Therefore, the proton spin rotation can be written as $R_y(\beta_{\Delta^*})$, with reversed Wigner angle sign

$$\beta_{\Delta^*} = \theta_p^{\Delta^*} + \theta_{\Delta^*} - \alpha_{\Delta^*}^W. \quad (65)$$

The decay amplitudes for each decay chain are the product of two two-body decay amplitudes, summed over the proton helicities for Λ^* and Δ^* chains,

$$\mathscr{A}_{\nu_{\Lambda_c^+}, m_p, \bar{\lambda}_{K^*}}^{K^*} = \mathscr{H}_{m_p, \bar{\lambda}_{K^*}}^{K^*} \delta_{\nu_{\Lambda_c^+}, m_p + \bar{\lambda}_{K^*}} d_{\bar{\lambda}_{K^*}, 0}^{*S_{K^*}}$$
$$\cdot \left(\bar{\theta}_K\right) \mathscr{R}_{K^*}\left(m_{K^-\pi^+}^2\right), \quad (66)$$

$$\mathscr{A}_{\nu_{\Lambda_c^+}, \lambda_{\Lambda^*}, m_p}^{\Lambda^*} = \sum_{\lambda_p^{\Lambda^*}} \mathscr{H}_{\lambda_{\Lambda^*}, 0}^{\Lambda^*} d_{\nu_{\Lambda_c^+}, \lambda_{\Lambda^*}}^{1/2}(\theta_{\Lambda^*}) d_{\lambda_{\Lambda^*}, \lambda_p^{\Lambda^*}}^{S_{\Lambda^*}}$$
$$\cdot \left(\theta_p^{\Lambda^*}\right) d_{m_p, \lambda_p^{\Lambda^*}}^{1/2}(\beta_{\Lambda^*}) \mathscr{R}_{\Lambda^*}\left(m_{pK^-}^2\right), \quad (67)$$

$$\mathscr{A}_{\nu_{\Lambda_c^+}, \lambda_{\Delta^*}, m_p}^{\Delta^{++*}} = \sum_{\lambda_p^{\Delta^*}} \mathscr{H}_{\lambda_{\Delta^*}, 0}^{\Delta^{++*}} d_{\nu_{\Lambda_c^+}, \lambda_{\Delta^*}}^{1/2}(\theta_{\Delta^*}) d_{\lambda_{\Delta^*}, \lambda_p^{\Delta^*}}^{S_{\Delta^*}}$$
$$\cdot \left(\theta_p^{\Delta^*}\right) d_{m_p, \lambda_p^{\Delta^*}}^{1/2}(\beta_{\Delta^*}) \mathscr{R}_{\Delta^*}\left(m_{p\pi^+}^2\right). \quad (68)$$

The complete amplitude for the $\Lambda_c^+ \longrightarrow pK^-\pi^+$ decay is obtained summing the amplitudes for all the intermediate resonances and their allowed helicity states,

$$\mathcal{O}_{\nu_{\Lambda_c^+}, m_p}\left(m_{pK^-}^2, m_{K^-\pi^+}^2\right) = \sum_{i=1}^{N_{K^*}} \sum_{\bar{\lambda}_{K^*}} \mathscr{A}_{\nu_{\Lambda_c^+}, m_p, \bar{\lambda}_{K^*}}^{\Lambda_c^+ \to K_i^*(\to K^-\pi^+)p}$$
$$+ \sum_{j=1}^{N_{\Lambda^*}} \sum_{\bar{\lambda}_{\Lambda^*}} \mathscr{A}_{\nu_{\Lambda_c^+}, \bar{\lambda}_{\Lambda^*}, m_p}^{\Lambda_c^+ \to \Lambda_j^*(\to pK^-)\pi^+} \quad (69)$$
$$+ \sum_{k=1}^{N_{\Delta^*}} \sum_{\lambda_{\Delta^{++*}}} \mathscr{A}_{\nu_{\Lambda_c^+}, \bar{\lambda}_{\Delta^*}, m_p}^{\Lambda_c^+ \to \Delta_k^{++*} K^-}.$$

5.4. Study of the Decay Rate. We divide the study of the decay rate into different parts, investigating which information each gives on the parameters describing the decay distribution. In particular, we will focus on helicity couplings and the polarisation degree. Each complex helicity coupling is

equivalent to two real parameters, its real and imaginary part or its modulus and phase. Therefore, we have two real unknowns for each coupling plus the polarisation modulus. Each part of the decay rate having a functional form distinguishable from the others via an amplitude fit yields a constraint on the combination of parameters involved in that contribution.

First, we study the part of the decay rate without interference terms, consisting of the sum of the rates associated to each single contribution. For the $\Lambda_c^+ \longrightarrow pK^-\pi^+$ decay, each contribution is given by Eq. (36), since intermediate resonances decay via parity conserving strong interaction,

$$p^{\text{non-int}}(\Omega, P_z)$$
$$= \sum_{i=1}^{N_{K^*}} \left(F_{K_i^*} + P_z \alpha_{K_i^*} \cos\theta_{K^*}\right) \left| g_{K_i^*}^{S_{K_i^*}}\left(m_{K^-\pi^+}^2, \theta_K\right)\right|^2$$
$$+ \sum_{j=1}^{N_{\Lambda^*}} \left(F_{\Lambda_j^*} + P_z \alpha_{\Lambda_j^*} \cos\theta_{\Lambda^*}\right) \left| g_{\Lambda_j^*}^{S_{\Lambda_j^*}}\left(m_{pK^-}^2, \theta_p^{\Lambda^*}\right)\right|^2$$
$$+ \sum_{k=1}^{N_{\Delta^*}} \left(F_{\Delta_k^*} + P_z \alpha_{\Delta_k^*} \cos\theta_{\Delta^*}\right) \left| g_{\Delta_j^*}^{S_{\Delta_k^*}}\left(m_{p\pi^+}^2, \theta_p^{\Delta^*}\right)\right|^2, \quad (70)$$

in which angles are defined in analogy with Eq. (36) and the F_R values are the sum of the helicity couplings squared moduli for the resonance R,

$$F_R \equiv \sum_{\lambda_1, \bar{\lambda}_2} \left| \mathscr{H}_{\lambda_1, \bar{\lambda}_2}^R \right|^2. \quad (71)$$

These are related to the resonance fit fractions $\mathscr{F}_R$ via

$$\mathscr{F}_R \equiv \int F_R \left| g_R^{S_R}\left(m_R^2, \theta_1^R\right)\right|^2 d\Omega. \quad (72)$$

The overall normalisation of the decay rate, ensuring it has unit integral over the phase space, is intended to be implicit in the definition of the helicity couplings.

The decay rate part without interference terms gives information on F_R and the products $P_z \alpha_R$, but, again, it does not allow to separate the polarisation modulus from the α values without an independent measurement of at least one of them.

For later convenience, let us evaluate the noninterfering decay rate part associated to a Λ^* resonance in the Dalitz plot amplitude decomposition. Starting from Eq. (67), its expression greatly simplifies exploiting the orthogonality of d-matrices,

$$\sum_{m_p} d_{m_p, \lambda_p^{\Lambda^*}}^{1/2}(\beta_{\Lambda^*}) d_{m_p, \lambda'_p^{\Lambda^*}}^{1/2}(\beta_{\Lambda^*}) = \delta_{\lambda_p^{\Lambda^*}, \lambda'_p^{\Lambda^*}},$$

$$\sum_{\lambda_p^{\Lambda^*}} d_{\lambda_{\Lambda^*}, \lambda_p^{\Lambda^*}}^{S_{\Lambda^*}}\left(\theta_p^{\Lambda^*}\right) = d_{\lambda_{\Lambda^*}, \lambda_p^{\Lambda^*}}^{S_{\Lambda^*}}\left(\theta_p^{\Lambda^*}\right) = \delta_{\lambda_{\Lambda^*}, \lambda_{\Lambda^*}'} f\left(S_{\Lambda^*}, \theta_p^{\Lambda^*}\right)^2,$$

$$(73)$$

obtaining

$$\sum_{m_p} \mathcal{O}^{\Lambda^*}_{\nu_{\Lambda_c^+}, m_p} \mathcal{O}^{*\Lambda^*}_{\nu'_{\Lambda_c^+}, m_p} = \sum_{\lambda_{\Lambda^*}} \left| \mathcal{H}^{\Lambda^*}_{\lambda_{\Lambda^*},0} \right|^2 d^{1/2}_{\nu_{\Lambda_c^+}, \lambda_{\Lambda^*}}(\theta_{\Lambda^*}) d^{1/2}_{\nu'_{\Lambda_c^+}, \lambda_{\Lambda^*}}(\theta_{\Lambda^*})$$
$$\cdot \left| g^{S_{\Lambda^*}}_{\Lambda^*}\left(m^2_{pK^-}, \theta^{\Lambda^*}_p\right)\right|^2. \tag{74}$$

Explicitly, we have

$$\sum_{m_p} \left| \mathcal{O}^{\Lambda^*}_{1/2, m_p}\right|^2 = \left(\left| \mathcal{H}^{\Lambda^*}_{1/2,0}\right|^2 \cos^2 \frac{\theta_{\Lambda^*}}{2} + \left| \mathcal{H}^{\Lambda^*}_{-1/2,0}\right|^2 \sin^2 \frac{\theta_{\Lambda^*}}{2} \right)$$
$$\cdot \left| g^{S_{\Lambda^*}}_{\Lambda^*}\left(m^2_{pK^-}, \theta^{\Lambda^*}_p\right)\right|^2,$$

$$\sum_{m_p} \mathcal{O}^{\Lambda^*}_{1/2, m_p} \mathcal{O}^{*\Lambda^*}_{-1/2, m_p} = \left(\left| \mathcal{H}^{\Lambda^*}_{1/2,0}\right|^2 - \left| \mathcal{H}^{\Lambda^*}_{-1/2,0}\right|^2 \right) \sin \frac{\theta_{\Lambda^*}}{2} \cos \frac{\theta_{\Lambda^*}}{2}$$
$$\times \left| g^{S_{\Lambda^*}}_{\Lambda^*}\left(m^2_{pK^-}, \theta^{\Lambda^*}_p\right)\right|^2 = \sum_{m_p} \mathcal{O}^{\Lambda^*}_{-1/2, m_p} \mathcal{O}^{*\Lambda^*}_{1/2, m_p},$$

$$\sum_{m_p} \left| \mathcal{O}^{\Lambda^*}_{-1/2, m_p}\right|^2 = \left(\left| \mathcal{H}^{\Lambda^*}_{1/2,0}\right|^2 \sin^2 \frac{\theta_{\Lambda^*}}{2} + \left| \mathcal{H}^{\Lambda^*}_{-1/2,0}\right|^2 \cos^2 \frac{\theta_{\Lambda^*}}{2} \right)$$
$$\cdot \left| g^{S_{\Lambda^*}}_{\Lambda^*}\left(m^2_{pK^-}, \theta^{\Lambda^*}_p\right)\right|^2. \tag{75}$$

The contribution to the unpolarised decay rate Eq. (40) is

$$p_{\text{unpol}}\left(m^2_{pK^-}, m^2_{K^-\pi^+}\right)$$
$$= \sum_{\nu_{\Lambda_c^+}, m_p} \left| \mathcal{O}^{\Lambda^*}_{\nu_{\Lambda_c^+}, m_p}\right|^2 = F_{\Lambda^*} \left| g^{S_{\Lambda^*}}_{\Lambda^*}\left(m^2_{pK^-}, \theta^{\Lambda^*}_p\right)\right|^2, \tag{76}$$

while the contribution to the longitudinal polarisation rate Eq. (42) is

$$p_{\text{long}}(\Omega, P_z) = P_z \left[\cos \theta_p \sum_{m_p} \left(\left| \mathcal{O}^{\Lambda^*}_{1/2, m_p}\right|^2 - \left| \mathcal{O}^{\Lambda^*}_{-1/2, m_p}\right|^2 \right) \right.$$
$$\left. - 2 \sin \theta_p \, \text{Re} \sum_{m_p} \exp i\chi \, \mathcal{O}^{\Lambda^*}_{1/2, m_p} \mathcal{O}^{*\Lambda^*}_{-1/2, m_p} \right]$$
$$= P_z \alpha_{\Lambda^*}\left(\cos \theta_p \cos \theta_{\Lambda^*} - \sin \theta_p \sin \theta_{\Lambda^*} \cos \chi \right)$$
$$\cdot \left| g^{S_{\Lambda^*}}_{\Lambda^*}\left(m^2_{pK^-}, \theta^{\Lambda^*}_p\right)\right|^2. \tag{77}$$

The above expressions are equivalent to Eq. (70), the only difference being in the choice of the angles describing the decay distributions. Indeed, the definition of the helicity angle θ_{Λ^*} is different in the two cases: while in Eqs. (76) and (77), it is independent of the decay orientation angles (θ_p, ϕ_p, χ); in Eq. (70), θ_{Λ^*} depends on a combination of invariant mass and decay orientation degrees of freedom.

Of course, nothing changes in terms of sensitivity to the decay parameters: the χ angle dependent term does not add information to the $\Lambda_c^+ \longrightarrow pK^-\pi^+$ decay parameters.

The Λ^* contribution is characterised by 4 unknowns related to couplings plus the polarisation modulus, which is shared with the other contributions. This part of the decay rate places two constraints determining the sum of the helicity coupling moduli and their relative difference up to the polarisation factor.

Now, we consider the interference terms between resonance contributions, showing in which way they allow to get maximum information on the decay amplitudes, constraining all the parameters describing the $\Lambda_c^+ \longrightarrow pK^-\pi^+$ decay distributions. There are two kinds of interference terms: those arising from resonances belonging to the same decay chain and those coming from resonances associated to different decay chains. In the following, we will consider one example for each type.

5.4.1. Interference Term $\Lambda^* - \Lambda'^*$. Let us consider the interference term between two Λ^* resonances. Its computation is analogous to the Λ^* decay rate, since both resonances belong to the same decay chain, sharing the same rotation angles,

$$\sum_{m_p} \mathcal{O}^{\Lambda^*}_{\nu_{\Lambda_c^+}, m_p} \mathcal{O}^{*\Lambda'^*}_{\nu'_{\Lambda_c^+}, m_p}$$
$$= \sum_{\lambda_{\Lambda^*}} \mathcal{H}^{\Lambda^*}_{\lambda_{\Lambda^*},0} \mathcal{H}^{*\Lambda'^*}_{\lambda_{\Lambda^*},0} d^{1/2}_{\nu_{\Lambda_c^+}, \lambda_{\Lambda^*}}(\theta_{\Lambda^*}) d^{1/2}_{\nu'_{\Lambda_c^+}, \lambda_{\Lambda^*}} \tag{78}$$
$$\cdot (\theta_{\Lambda^*}) G^{S_{\Lambda^*}, S_{\Lambda'^*}}_{\Lambda^*, \Lambda'^*}\left(m^2_{pK^-}, \theta^{\Lambda^*}_p\right),$$

in which

$$G^{S_{\Lambda^*}, S_{\Lambda'^*}}_{\Lambda^*, \Lambda'^*}\left(m^2_{pK^-}, \theta^{\Lambda^*}_p\right)$$
$$\equiv f\left(S_{\Lambda^*}, \theta^{\Lambda^*}_p\right) f\left(S_{\Lambda'^*}, \theta^{\Lambda^*}_p\right) \mathcal{R}_{\Lambda^*}\left(m^2_{pK^-}\right) \mathcal{R}_{\Lambda'^*}\left(m^2_{pK^-}\right). \tag{79}$$

Explicitly (leaving out G function arguments),

$$\sum_{m_p} \mathcal{O}^{\Lambda^*}_{1/2, m_p} \mathcal{O}^{*\Lambda'^*}_{1/2, m_p} = \left(\mathcal{H}^{\Lambda^*}_{1/2,0} \mathcal{H}^{*\Lambda'^*}_{1/2,0} \cos^2 \frac{\theta_{\Lambda^*}}{2} + \mathcal{H}^{\Lambda^*}_{-1/2,0} \mathcal{H}^{*\Lambda'^*}_{-1/2,0} \sin^2 \frac{\theta_{\Lambda^*}}{2} \right) G,$$

$$\sum_{m_p} \mathcal{O}^{\Lambda^*}_{1/2, m_p} \mathcal{O}^{*\Lambda'^*}_{-1/2, m_p} = \left(\mathcal{H}^{\Lambda^*}_{1/2,0} \mathcal{H}^{*\Lambda'^*}_{1/2,0} - \mathcal{H}^{\Lambda^*}_{-1/2,0} \mathcal{H}^{*\Lambda'^*}_{-1/2,0} \right) \sin \frac{\theta_{\Lambda^*}}{2} \cos \frac{\theta_{\Lambda^*}}{2} G$$
$$= \sum_{m_p} \mathcal{O}^{\Lambda^*}_{-1/2, m_p} \mathcal{O}^{*\Lambda'^*}_{1/2, m_p},$$

$$\sum_{m_p} \mathcal{O}^{\Lambda^*}_{-1/2, m_p} \mathcal{O}^{*\Lambda'^*}_{-1/2, m_p} = \left(\mathcal{H}^{\Lambda^*}_{1/2,0} \mathcal{H}^{*\Lambda'^*}_{1/2,0} \sin^2 \frac{\theta_{\Lambda^*}}{2} + \mathcal{H}^{\Lambda^*}_{-1/2,0} \mathcal{H}^{*\Lambda'^*}_{-1/2,0} \cos^2 \frac{\theta_{\Lambda^*}}{2} \right) G. \tag{80}$$

Let us consider the contribution of this interference term to the decay rate, including its complex conjugate

corresponding to the exchange $\Lambda^* \leftrightarrow \Lambda'^*$. The unpolarised decay rate part Eq. (40) is

$$p_{\text{unpol}}\left(m_{pK^-}^2, m_{K^-\pi^+}^2\right) = 2 \operatorname{Re} \sum_{\nu_{\Lambda_c^+}, m_p} \mathcal{O}_{\nu_{\Lambda_c^+}, m_p}^{\Lambda^*} \mathcal{O}_{\nu_{\Lambda_c^+}, m_p}^{\Lambda'^*}$$
$$= 2 \operatorname{Re}\left(F_{\Lambda^*\Lambda'^*} G\right),$$
(81)

while the longitudinal polarisation part Eq. (42) is

$$p_{\text{long}}(\Omega, P_z)$$
$$= P_z \Bigg\{ \cos\theta_p 2 \operatorname{Re} \sum_{m_p} \left(\mathcal{O}_{1/2,m_p}^{\Lambda^*} \mathcal{O}_{1/2,m_p}^{\Lambda'^*} - \mathcal{O}_{-1/2,m_p}^{\Lambda^*} \mathcal{O}_{-1/2,m_p}^{\Lambda'^*} \right)$$
$$- 2\sin\theta_p \operatorname{Re} \sum_{m_p} \left[\exp i\chi \left(\mathcal{O}_{1/2,m_p}^{\Lambda^*} \mathcal{O}_{-1/2,m_p}^{\Lambda'^*} + \mathcal{O}_{-1/2,m_p}^{\Lambda^*} \mathcal{O}_{1/2,m_p}^{\Lambda'^*} \right) \right] \Bigg\}$$
$$= 2P_z \big[\cos\theta_p \cos\theta_{\Lambda^*} \operatorname{Re}\left(\alpha_{\Lambda^*\Lambda'^*} G\right) - \sin\theta_p \sin\theta_{\Lambda^*} \operatorname{Re}$$
$$\times \left(\exp i\chi \alpha_{\Lambda^*\Lambda'^*} G \right) \big],$$
(82)

which probe the combinations

$$F_{\Lambda^*\Lambda'^*} \equiv \mathcal{H}_{1/2,0}^{\Lambda^*} \mathcal{H}_{1/2,0}^{*\Lambda'^*} + \mathcal{H}_{-1/2,0}^{\Lambda^*} \mathcal{H}_{-1/2,0}^{*\Lambda'^*},$$
$$\alpha_{\Lambda^*\Lambda'^*} \equiv \mathcal{H}_{1/2,0}^{\Lambda^*} \mathcal{H}_{1/2,0}^{*\Lambda'^*} + \mathcal{H}_{-1/2,0}^{\Lambda^*} \mathcal{H}_{-1/2,0}^{*\Lambda'^*}.$$
(83)

The structure of this interference term is similar to the Λ^* decay rate: a $F_{\Lambda^*\Lambda'^*}$ term probed by the unpolarised decay rate and a polarisation-dependent term driven by a parity-violating asymmetry parameter $\alpha_{\Lambda^*\Lambda'^*}$.

To better study the constraints given by this interference term, let us write both complex couplings and the G function in modulus-phase decomposition,

$$\mathcal{H}_{1/2,0}^{\Lambda^*} = P_{1/2,0}^{\Lambda^*} \exp i\Phi_{1/2,0}^{\Lambda^*},$$
$$G = |G| \exp i\phi_G.$$
(84)

We have

$$\operatorname{Re}\left(F_{\Lambda^*\Lambda'^*} G\right)/|G|$$
$$= P_{1/2,0}^{\Lambda^*} P_{1/2,0}^{\Lambda'^*} \cos\left(\Phi_{1/2,0}^{\Lambda^*} - \Phi_{1/2,0}^{\Lambda'^*} + \phi_G\right)$$
$$+ P_{-1/2,0}^{\Lambda^*} P_{-1/2,0}^{\Lambda'^*} \cos\left(\Phi_{-1/2,0}^{\Lambda^*} - \Phi_{-1/2,0}^{\Lambda'^*} + \phi_G\right),$$

$$P_z \operatorname{Re}\left(\alpha_{\Lambda^*\Lambda'^*} G\right)/|G|$$
$$= P_z P_{1/2,0}^{\Lambda^*} P_{1/2,0}^{\Lambda'^*} \cos\left(\Phi_{1/2,0}^{\Lambda^*} - \Phi_{1/2,0}^{\Lambda'^*} + \phi_G\right)$$
$$- P_z P_{-1/2,0}^{\Lambda^*} P_{-1/2,0}^{\Lambda'^*} \cos\left(\Phi_{-1/2,0}^{\Lambda^*} - \Phi_{-1/2,0}^{\Lambda'^*} + \phi_G\right)$$
(85)

Since the phase ϕ_G has in general a nontrivial dependence on the resonance invariant mass (e.g., relativistic

Breit-Wigner lineshapes have such behaviour), the two conditions place four constraints on decay parameters: indeed one has

$$\cos\left(\Phi_{1/2,0}^{\Lambda^*} - \Phi_{1/2,0}^{\Lambda'^*} + \phi_G\right)$$
$$= \cos\left(\Phi_{1/2,0}^{\Lambda^*} - \Phi_{1/2,0}^{\Lambda'^*}\right) \cos\phi_G$$
$$- \sin\left(\Phi_{1/2,0}^{\Lambda^*} - \Phi_{1/2,0}^{\Lambda'^*} + \right) \sin\phi_G,$$
(86)

showing that phase differences among couplings can be probed, not only their cosine, since $\cos\phi_G$ and $\sin\phi_G$ functional forms are separable by an amplitude fit. The constraint given by the χ-dependent term is redundant.

Considering the decay rate part associated to Λ and Λ'^* resonances, we have 9 unknowns (8 real couplings + P_z) and 8 constraints (4 from single decay rates + 4 from the interference term): again, we miss a condition to determine separately the set of helicity couplings and the polarisation.

What happens if we consider a set of three interfering Λ^* resonances? We have 13 unknowns and 16 constraints (now 12 coming from the three interference terms) and therefore the possibility to measure both the full set of helicity couplings and the polarisation. Practically, to have significant interference effects the three resonances must feature a significant overlap in invariant mass dependence (otherwise the lineshape product $\mathcal{R}_{\Lambda^*}(m_{pK^-}^2)\mathcal{R}_{\Lambda'^*}(m_{pK^-}^2)$ vanishes) which can make their separation in the amplitude fit difficult, especially if they have the same spin.

5.4.2. Interference Term $\Lambda^* - \Delta^*$. Let us consider the interference term between one Λ^* and one Δ^* resonance. Starting from Eqs. (67) and (68), its expression is

$$\sum_{m_p} \mathcal{O}_{\nu_{\Lambda_c^+}, m_p}^{\Lambda^*} \mathcal{O}_{\nu_{\Lambda_c^+}', m_p}^{*\Delta^*}$$
$$= \sum_{m_p} \sum_{\lambda_{\Lambda^*}} \mathcal{H}_{\lambda_{\Lambda^*},0}^{\Lambda^*} d_{\nu_{\Lambda_c^+}, \lambda_{\Lambda^*}}^{1/2}(\theta_{\Lambda^*}) d_{\lambda_{\Lambda^*}, \lambda_p^{\Lambda^*}}^{S_{\Lambda^*}}\left(\theta_p^{\Lambda^*}\right) d_{m_p, \lambda_p^{\Lambda^*}}^{1/2}(\beta_{\Lambda^*})$$
$$\times \sum_{\lambda_{\Delta^*}} \mathcal{H}_{\lambda_{\Delta^*},0}^{\Delta^*} d_{\nu_{\Lambda_c^+}', \lambda_{\Delta^*}}^{1/2}(\theta_{\Delta^*}) d_{\lambda_{\Delta^*}, \lambda_p^{\Delta^*}}^{S_{\Delta^*}}\left(\theta_p^{\Delta^*}\right) d_{m_p, \lambda_p^{\Delta^*}}^{1/2}(\beta_{\Delta^*})$$
$$\times G_{\Lambda^*, \Delta^*}^{S_{\Lambda^*}, S_{\Delta^*}}\left(m_{pK^-}^2, m_{p\pi^+}^2, \theta_p^{\Lambda^*}, \theta_p^{\Delta^*}\right),$$
(87)

with

$$G_{\Lambda^*, \Delta^*}^{S_{\Lambda^*}, S_{\Delta^*}}\left(m_{pK^-}^2, m_{p\pi^+}^2, \theta_p^{\Lambda^*}, \theta_p^{\Delta^*}\right)$$
$$\equiv f\left(S_{\Lambda^*}, \theta_p^{\Lambda^*}\right) f\left(S_{\Delta^*}, \theta_p^{\Delta^*}\right) \mathcal{R}_{\Lambda^*}\left(m_{pK^-}^2\right) \mathcal{R}_{\Delta^*}\left(m_{p\pi^+}^2\right).$$
(88)

This interference term is more complicated than the previous one since the two resonances belong to different decay chains, characterised by different rotation angles. However, trigonometric functions arrange in such a way the proton rotation angles enter the decay rate only via the combination

$$\gamma \equiv \frac{\theta_p^{\Lambda^*} - \theta_p^{\Delta^*} - \beta_{\Lambda^*} + \beta_{\Delta^*}}{2}. \tag{89}$$

Explicitly (leaving out function arguments),

$$\sum_{m_p} \mathcal{O}_{1/2,m_p}^{\Lambda^*} \mathcal{O}_{1/2,m_p}^{*\Delta^*} = \left[\mathcal{H}_{1/2,0}^{\Lambda^*} \mathcal{H}_{1/2,0}^{*\Delta^*} \cos\frac{\theta_{\Lambda^*}}{2} \cos\frac{\theta_{\Delta^*}}{2} \cos\gamma \right.$$
$$+ \mathcal{H}_{1/2,0}^{\Lambda^*} \mathcal{H}_{-1/2,0}^{*\Delta^*} \cos\frac{\theta_{\Lambda^*}}{2} \sin\frac{\theta_{\Delta^*}}{2} \sin\gamma$$
$$- \mathcal{H}_{-1/2,0}^{\Lambda^*} \mathcal{H}_{1/2,0}^{*\Delta^*} \sin\frac{\theta_{\Lambda^*}}{2} \cos\frac{\theta_{\Delta^*}}{2} \sin\gamma$$
$$\left. + \mathcal{H}_{-1/2,0}^{\Lambda^*} \mathcal{H}_{-1/2,0}^{*\Delta^*} \sin\frac{\theta_{\Lambda^*}}{2} \sin\frac{\theta_{\Delta^*}}{2} \cos\gamma \right] G,$$

$$\sum_{m_p} \mathcal{O}_{1/2,m_p}^{\Lambda^*} \mathcal{O}_{-1/2,m_p}^{*\Delta^*} = \left[\mathcal{H}_{1/2,0}^{\Lambda^*} \mathcal{H}_{1/2,0}^{*\Delta^*} \cos\frac{\theta_{\Lambda^*}}{2} \sin\frac{\theta_{\Delta^*}}{2} \cos\gamma \right.$$
$$- \mathcal{H}_{1/2,0}^{\Lambda^*} \mathcal{H}_{-1/2,0}^{*\Delta^*} \cos\frac{\theta_{\Lambda^*}}{2} \cos\frac{\theta_{\Delta^*}}{2} \sin\gamma$$
$$- \mathcal{H}_{-1/2,0}^{\Lambda^*} \mathcal{H}_{1/2,0}^{*\Delta^*} \sin\frac{\theta_{\Lambda^*}}{2} \sin\frac{\theta_{\Delta^*}}{2} \sin\gamma$$
$$\left. + \mathcal{H}_{-1/2,0}^{\Lambda^*} \mathcal{H}_{-1/2,0}^{*\Delta^*} \sin\frac{\theta_{\Lambda^*}}{2} \cos\frac{\theta_{\Delta^*}}{2} \cos\gamma \right] G,$$

$$\sum_{m_p} \mathcal{O}_{-1/2,m_p}^{\Lambda^*} \mathcal{O}_{1/2,m_p}^{*\Delta^*} = \left[\mathcal{H}_{1/2,0}^{\Lambda^*} \mathcal{H}_{1/2,0}^{*\Delta^*} \sin\frac{\theta_{\Lambda^*}}{2} \cos\frac{\theta_{\Delta^*}}{2} \cos\gamma \right.$$
$$+ \mathcal{H}_{1/2,0}^{\Lambda^*} \mathcal{H}_{-1/2,0}^{*\Delta^*} \sin\frac{\theta_{\Lambda^*}}{2} \sin\frac{\theta_{\Delta^*}}{2} \sin\gamma$$
$$+ \mathcal{H}_{-1/2,0}^{\Lambda^*} \mathcal{H}_{1/2,0}^{*\Delta^*} \cos\frac{\theta_{\Lambda^*}}{2} \cos\frac{\theta_{\Delta^*}}{2} \sin\gamma$$
$$\left. + \mathcal{H}_{-1/2,0}^{\Lambda^*} \mathcal{H}_{-1/2,0}^{*\Delta^*} \cos\frac{\theta_{\Lambda^*}}{2} \sin\frac{\theta_{\Delta^*}}{2} \cos\gamma \right] G,$$

$$\sum_{m_p} \mathcal{O}_{-1/2,m_p}^{\Lambda^*} \mathcal{O}_{-1/2,m_p}^{*\Delta^*} = \left[\mathcal{H}_{1/2,0}^{\Lambda^*} \mathcal{H}_{1/2,0}^{*\Delta^*} \sin\frac{\theta_{\Lambda^*}}{2} \sin\frac{\theta_{\Delta^*}}{2} \cos\gamma \right.$$
$$- \mathcal{H}_{1/2,0}^{\Lambda^*} \mathcal{H}_{-1/2,0}^{*\Delta^*} \sin\frac{\theta_{\Lambda^*}}{2} \cos\frac{\theta_{\Delta^*}}{2} \sin\gamma$$
$$+ \mathcal{H}_{-1/2,0}^{\Lambda^*} \mathcal{H}_{1/2,0}^{*\Delta^*} \cos\frac{\theta_{\Lambda^*}}{2} \sin\frac{\theta_{\Delta^*}}{2} \sin\gamma$$
$$\left. + \mathcal{H}_{-1/2,0}^{\Lambda^*} \mathcal{H}_{-1/2,0}^{*\Delta^*} \cos\frac{\theta_{\Lambda^*}}{2} \cos\frac{\theta_{\Delta^*}}{2} \cos\gamma \right] G. \tag{90}$$

TABLE 1: Summary of the $\Lambda_c^+ \to pK^-\pi^+$ decay rate study. It is reported which part of the decay rate is necessary to get information on the model parameters under which conditions. See text for details.

Quantity	Decay rate part	Requirements
$F_R, \mathscr{F}_R$	Noninterfering	
α_R	Noninterfering	$|P| > 0$
$F_{RR'}$	Interference $R - R'$	
$\alpha_{RR'}$	Interference $R - R'$	$|P| > 0$
$\mathscr{H}^R$	Interference $R - R' - R''$	$|P| > 0$
	Interference $R - S$	$|P| > 0$
$\hat{P}$	Noninterfering	Parity-violation
$|P|$	Interference $R - R' - R''$	Parity-violation
	Interference $R - S$	Parity-violation

The contribution to the unpolarised decay rate Eq. (40) is

$$p_{unpol}\left(m_{pK^-}^2, m_{K^-\pi^+}^2\right)$$
$$= 2\,\mathrm{Re} \sum_{\nu_{\Lambda_c^+}, m_p} \mathcal{O}_{\nu_{\Lambda_c^+}, m_p}^{\Lambda^*} \mathcal{O}_{\nu'_{\Lambda_c^+}, m_p}^{*\Lambda^*}$$
$$= 2\,\mathrm{Re}\left[\left(\mathcal{H}_{1/2,0}^{\Lambda^*} \mathcal{H}_{1/2,0}^{*\Delta^*} + \mathcal{H}_{-1/2,0}^{\Lambda^*} \mathcal{H}_{-1/2,0}^{*\Delta^*} \right) \cos\left(\frac{\theta_{\Lambda^*} - \theta_{\Delta^*}}{2}\right) \cos\gamma \right.$$
$$\left. - \left(\mathcal{H}_{1/2,0}^{\Lambda^*} \mathcal{H}_{-1/2,0}^{*\Delta^*} + \mathcal{H}_{-1/2,0}^{\Lambda^*} \mathcal{H}_{1/2,0}^{*\Delta^*} \right) \sin\left(\frac{\theta_{\Lambda^*} - \theta_{\Delta^*}}{2}\right) \sin\gamma \right] G, \tag{91}$$

and that to the χ-independent longitudinal polarisation rate (the χ-dependent term does not add information on the parameters) is

$$p_{long}(\Omega, P_z)$$
$$= P_z \cos\theta_p 2\,\mathrm{Re} \sum_{m_p} \left(\mathcal{O}_{1/2,m_p}^{\Lambda^*} \mathcal{O}_{1/2,m_p}^{*\Lambda^*} - \mathcal{O}_{-1/2,m_p}^{\Lambda^*} \mathcal{O}_{-1/2,m_p}^{*\Lambda^*} \right)$$
$$= P_z \cos\theta_p 2\,\mathrm{Re}\left[\left(\mathcal{H}_{1/2,0}^{\Lambda^*} \mathcal{H}_{1/2,0}^{*\Delta^*} - \mathcal{H}_{-1/2,0}^{\Lambda^*} \mathcal{H}_{-1/2,0}^{*\Delta^*} \right) \cos \right.$$
$$\cdot \left(\frac{\theta_{\Lambda^*} + \theta_{\Delta^*}}{2} \right) \cos\gamma + \left(\mathcal{H}_{1/2,0}^{\Lambda^*} \mathcal{H}_{-1/2,0}^{*\Delta^*} - \mathcal{H}_{-1/2,0}^{\Lambda^*} \mathcal{H}_{1/2,0}^{*\Delta^*} \right)$$
$$\left. \cdot \sin\left(\frac{\theta_{\Lambda^*} + \theta_{\Delta^*}}{2} \right) \sin\gamma \right] G. \tag{92}$$

Following the discussion about the constraints placed by the $\Lambda^* - \Lambda'^*$ term, Section 5.4.1, each angular term determines the relative phase of each combination of helicity couplings, each corresponding to two constraints on real parameters, as from Eq. (86). Considering the

TABLE 2: Toy amplitude fit study for nonzero polarisation ($P_z = 0.5$). For helicity couplings, the two uncertainties are associated to their real and imaginary part separately.

Parameter	Generated value	Fitted value	Uncertainty	Starting value
K^*				
$\mathscr{H}_{1/2,0}$	1			
$\mathscr{H}_{1/2,-1}$	$0.5 + 0.5i$	$0.482 + 0.4956i$	$0.012 ; 0.0087$	1
$\mathscr{H}_{-1/2,1}$	i	$-0.019 + 1.0047i$	$0.019 ; 0.0088$	1
$\mathscr{H}_{-1/2,0}$	$-0.5 - 0.5i$	$-0.480 - 0.526i$	$0.014 ; 0.011$	1
m(GeV)	0.9	0.89980	0.00042	1.1
Γ(GeV)	0.2	0.1984	0.0014	0.1
Λ^*				
$\mathscr{H}_{-1/2,0}$	i	$-0.036 + 1.009i$	$0.017 ; 0.014$	1
$\mathscr{H}_{1/2,0}$	$0.8 - 0.4i$	$0.811 - 0.375i$	$0.011 ; 0.013$	1
m(GeV)	1.6	1.60129	0.00069	1.8
Γ(GeV)	0.2	0.2014	0.0015	0.3
Δ^*				
$\mathscr{H}_{-1/2,0}$	$0.6 - 0.4i$	$0.625 - 0.398i$	$0.011 ; .0.011$	1
$\mathscr{H}_{1/2,0}$	$0.1i$	$0.0034 + 0.1191i$	$0.0066 ; 0.0070$	1
m(GeV)	1.4	1.3994	0.0012	1.6
Γ(GeV)	0.2	0.2064	0.0023	0.1
$\boldsymbol{P}$				
P_z	0.5	0.5029	0.0038	0
P_x	0.	-0.0029	0.0036	0
P_y	0.	0.0015	0.0036	0

decay rate part associated to Λ and Δ^* resonances, we have 9 unknowns (8 real couplings + P_z) and 12 constraints (4 from single decay rates +8 from the interference term); it is therefore possible to measure separately each parameter characterising the decay rate: real and imaginary parts of the complex couplings and the polarisation degree, if the latter is nonzero. Interference effects between different decay channels are more important than those in the same decay channel, the firsts giving more information on the amplitude model parameters.

In the absence of polarisation, the constraints given by the unpolarised decay rate are insufficient to fully constrain helicity coupling values, as from the discussion in Section 2.2. These results are numerically cross-checked by means of the toy amplitude fit presented in Section 6.

5.4.3. Summary. In the following, we summarize the results of the study of the $\Lambda_c^+ \longrightarrow pK^-\pi^+$ decay rate, focusing on which part of the decay rate gives information on which amplitude model parameter, Table 1.

The sum of the helicity coupling moduli F_R for each resonance (hence the fit fraction $\mathscr{F}_R$) can be measured

from the decay rate without interference. The decay asymmetry parameters can be extracted from the same term but only in the presence of a significant polarisation degree.

The sum of helicity coupling products $F_{RR'}$ characterising the interference between resonances belonging to the same decay channel can be measured in the absence of polarisation, while the difference $\alpha_{RR'}$ needs nonzero polarisation.

The single helicity coupling complex values can be measured if their associate resonance has a significant interference with other two belonging to the same decay channel or one belonging to a different decay channel.

Assuming nonnegligible parity-violation effects, the polarisation direction $\hat{\boldsymbol{P}}$ can be measured from the non-interfering decay rate, as following from the two-body decay rate for generic polarisation Eq. (24). Instead, the polarisation modulus $|\boldsymbol{P}|$ can be determined separately from the helicity couplings only in the presence of significant interference among three resonances in the same decay channel or two belonging to different decay channels.

According to the ongoing $\Lambda_c^+ \longrightarrow pK^-\pi^+$ amplitude analysis from semileptonic decays at the LHCb experiment [1],
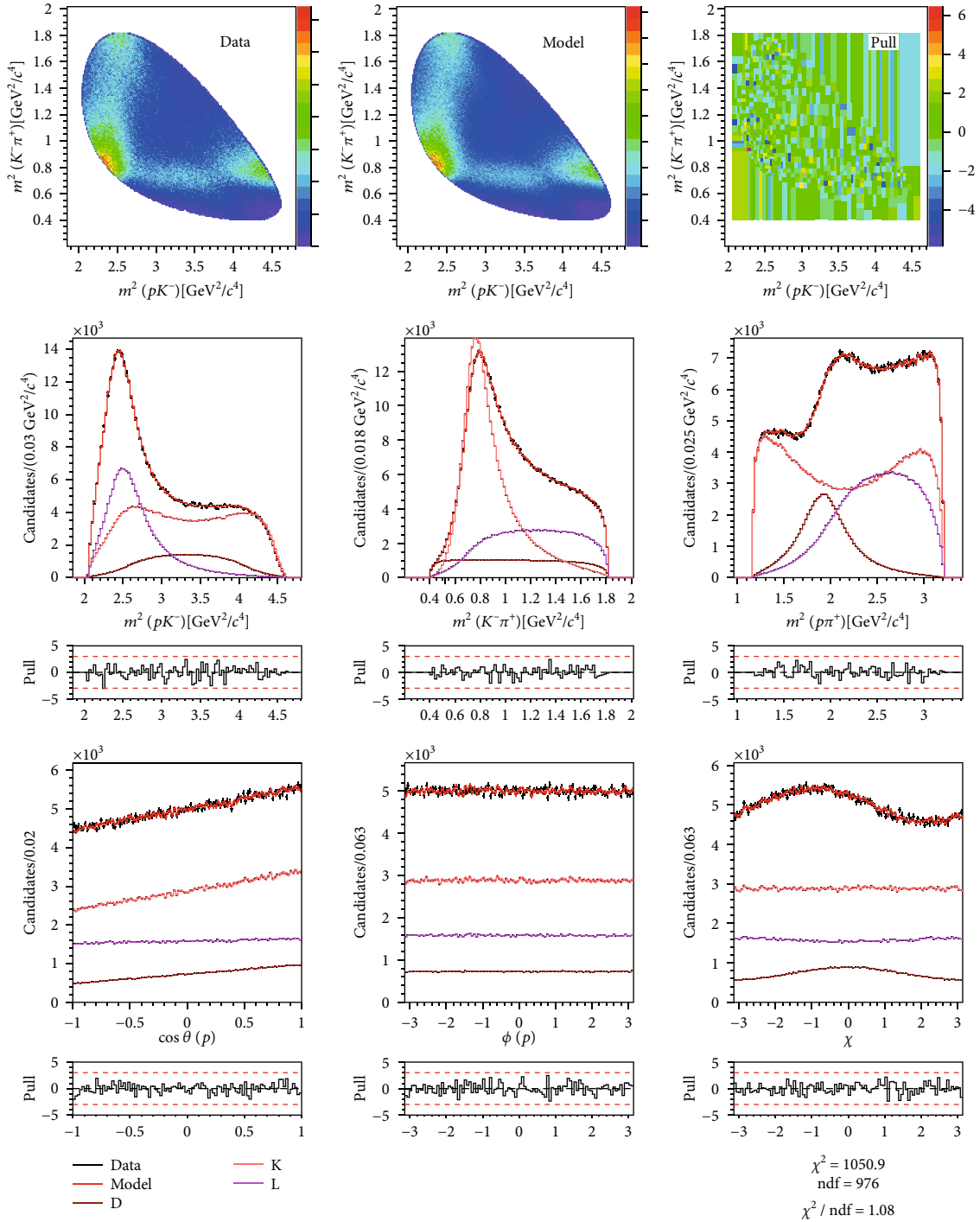
FIGURE 1: Comparison between Monte Carlo pseudodata ("Data") and fitted toy amplitude model ("Model") projections for nonzero polarisation ($P_z = 0.5$), summarized in Table 2.

all the requirements needed for extracting maximum information from $\Lambda_c^+ \longrightarrow pK^-\pi^+$ decay distributions are met: nonzero Λ_c^+ polarisation produced in the parent beauty hadron weak decay, significant parity-violation and resonant contributions in all its three decay channels with sizeable interference effects.

6. Toy Amplitude Fit

A toy amplitude maximum-likelihood fit is built to cross-check the results of the analytical study of the $\Lambda_c^+ \longrightarrow pK^-\pi^+$ decay rate presented in Section 5.4. We choose a toy amplitude model which satisfies the conditions summarized

TABLE 3: Toy amplitude fit study for zero polarisation. For helicity couplings, the two uncertainties are associated to their real and imaginary part separately.

Parameter	Generated value	Fitted value	Uncertainty	Starting value
K^*				
$\mathscr{H}_{1/2,0}$	1			
$\mathscr{H}_{1/2,-1}$	$0.5 + 0.5i$	$1.72 - 0.22i$	$0.12\,;0.17$	1
$\mathscr{H}_{-1/2,1}$	i	$0.732 + 0.27i$	$0.091\,;0.29$	1
$\mathscr{H}_{-1/2,0}$	$-0.5 - 0.5i$	$-1.01 - 1.29i$	$0.16\,;0.13$	1
m(GeV)	0.9	0.90060	0.00061	1.1
Γ(GeV)	0.2	0.2002	0.0019	0.1
Λ^*				
$\mathscr{H}_{-1/2,0}$	i	$-0.18 + 0.726i$	$0.13\,;0.053$	1
$\mathscr{H}_{1/2,0}$	$0.8 - 0.4i$	$1.65 - 1.09i$	$0.12\,;0.17$	1
m(GeV)	1.6	1.6016	0.0011	1.8
Γ(GeV)	0.2	0.2006	0.0017	0.3
Δ^*				
$\mathscr{H}_{-1/2,0}$	$0.6 - 0.4i$	$0.667 - 0.809i$	$0.083\,;.0.075$	1
$\mathscr{H}_{1/2,0}$	$0.1i$	$-0.419 - 0.240i$	$0.067\,;0.059$	1
m(GeV)	1.4	1.3969	0.0019	1.6
Γ(GeV)	0.2	0.2037	0.0040	0.1
P				
P_z	0	-0.0038	0.0034	0
P_x	0.	-0.0005	0.0035	0
P_y	0.	0.0005	0.0034	0

in Section 5.4.3; it consists of three resonances, one per decay channel, with resonance parameters and helicity couplings chosen in order to produce significant parity-violation and interference effects. Resonance lineshapes are taken to be relativistic Breit-Wigner functions [28],

$$\mathscr{R}_{BW}\left(m^2\right) = \frac{1}{m_0^2 - m^2 - im_0\Gamma_0}, \qquad (93)$$

characterised by mass m_0 and width Γ parameters. The following spin-parity J^P assignments are considered: $K^*(1^+)$, $\Lambda^*(1/2^-)$ and $\Delta^*(1/2^-)$.

The amplitude fit code is based on a version of the TensorFlowAnalysis package [29] adapted to five-dimensional phase space three-body amplitude fits [1]; this package depends on the machine-learning framework TensorFlow [30] interfaced with MINUIT minimisation [31] via the ROOT package [32].

A set of 500,000 Monte Carlo pseudodata has been generated according to the toy amplitude model, with the set of parameters reported in Table 2. For computational reasons, the helicity couplings are defined relatively

to a reference one, $\mathscr{H}_{1/2,0}^{K^*}$, whose value is fixed to 1. The normalisation of the decay rate is ensured computing its integral as a function of the fit parameters. The pseudodata sample is then fit with the same toy amplitude model leaving helicity couplings (but the reference one), polarisation components, and resonance masses and widths as free fit parameters. The starting and final values of the fit parameters are reported in Table 2, in which uncertainties are computed from the Hessian matrix associated to the maximum-likelihood fit. The starting point in parameter space is chosen to be far enough from the generated one, so that the possibility to obtain the generated values just by chance is negligible.

The fit results demonstrate that the amplitude fit is able to measure simultaneously all the amplitude model parameters: complex helicity couplings, polarisation degree and direction, and resonance masses and widths, as predicted by the analytical study of the $\Lambda_c^+ \longrightarrow pK^-\pi^+$ decay rate. Indeed, all the parameters are found to be compatible within twice the range set by the computed statistical uncertainties. The comparison between pseudodata and amplitude model projections is displayed in Figure 1.

To highlight the importance of having a nonzero polarisation for extracting full information from $\Lambda_c^+ \longrightarrow pK^-\pi^+$ decay distributions, we repeat the toy amplitude fit, exactly in the same way, but for pseudodata generated for zero polarisation. The results are reported in Table 3, while the null polarisation and resonance parameters are correctly retrieved, the helicity coupling values are far from the generated ones; their associated uncertainties, much larger than those characterising the previous fit, suggest that they are not fully constrained by the pseudodata distributions. The comparison between pseudodata and amplitude model projections is displayed in Figure 2.

What about the extraction of the fit fractions, which, according to Eq. (70), should be measurable even in the absence of polarisation? Due to the way the helicity couplings are defined in the amplitude fit, we should not check whether the sum of the helicity coupling moduli is retrieved, but rather the relative sum with respect to the other resonances. Indeed, from the final helicity coupling values reported in Table 3, it is easy to check that the F_R values are compatible with the generated ones but for an overall factor ≈ 2.5, which is absorbed in the amplitude model normalisation.

7. Conclusions

We perform an analytical study of the $\Lambda_c^+ \longrightarrow pK^-\pi^+$ decay to understand which information can be extracted from its decay distributions. This study holds as well for any three-body decay with spin structure $1/2 \longrightarrow 1/2\,0\,0$, having a first parity-violating decay to an intermediate state subsequently decaying via parity-conserving interactions.

Considering an amplitude model for the $\Lambda_c^+ \longrightarrow pK^-\pi^+$ decay written in the helicity formalism, we show which parameters of the amplitude model can be measured from which part of the decay rate. We demonstrate how the
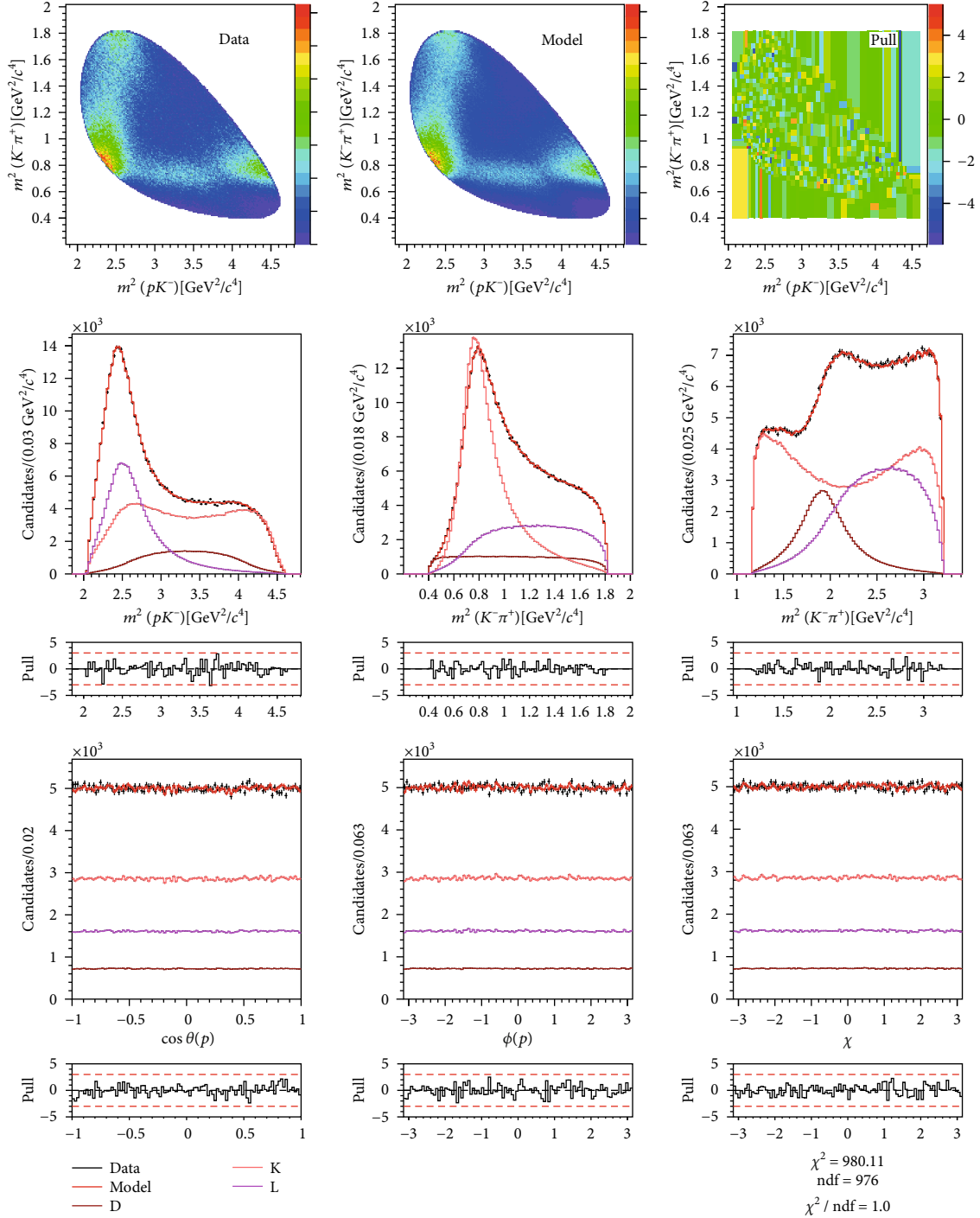
FIGURE 2: Comparison between Monte Carlo pseudodata ("Data") and fitted toy amplitude model ("Model") projections for zero polarisation, summarized in Table 2.

presence of significant interference effects together with a nonnegligible Λ_c^+ polarisation allows the simultaneous measurement of all the amplitude model parameters, including complex helicity couplings, and the polarisation degree and direction. We highlight the interplay between amplitude model and polarisation degree; significant resonance interference effects are needed to measure the second, while a nonzero polarisation allows to fully determine the decay model.

The analytical study has been cross-checked numerically by means of toy amplitude fits on Monte Carlo pseudodata.

According to the ongoing studies of $\Lambda_c^+ \longrightarrow pK^-\pi^+$ decays at LHCb [1], this decay has all the features needed for the complete determination of its amplitude model parameters. The full determination of the $\Lambda_c^+ \longrightarrow pK^-\pi^+$ amplitude model opens the possibility to use a $\Lambda_c^+ \longrightarrow pK^- \pi^+$ decay amplitude model for the different applications
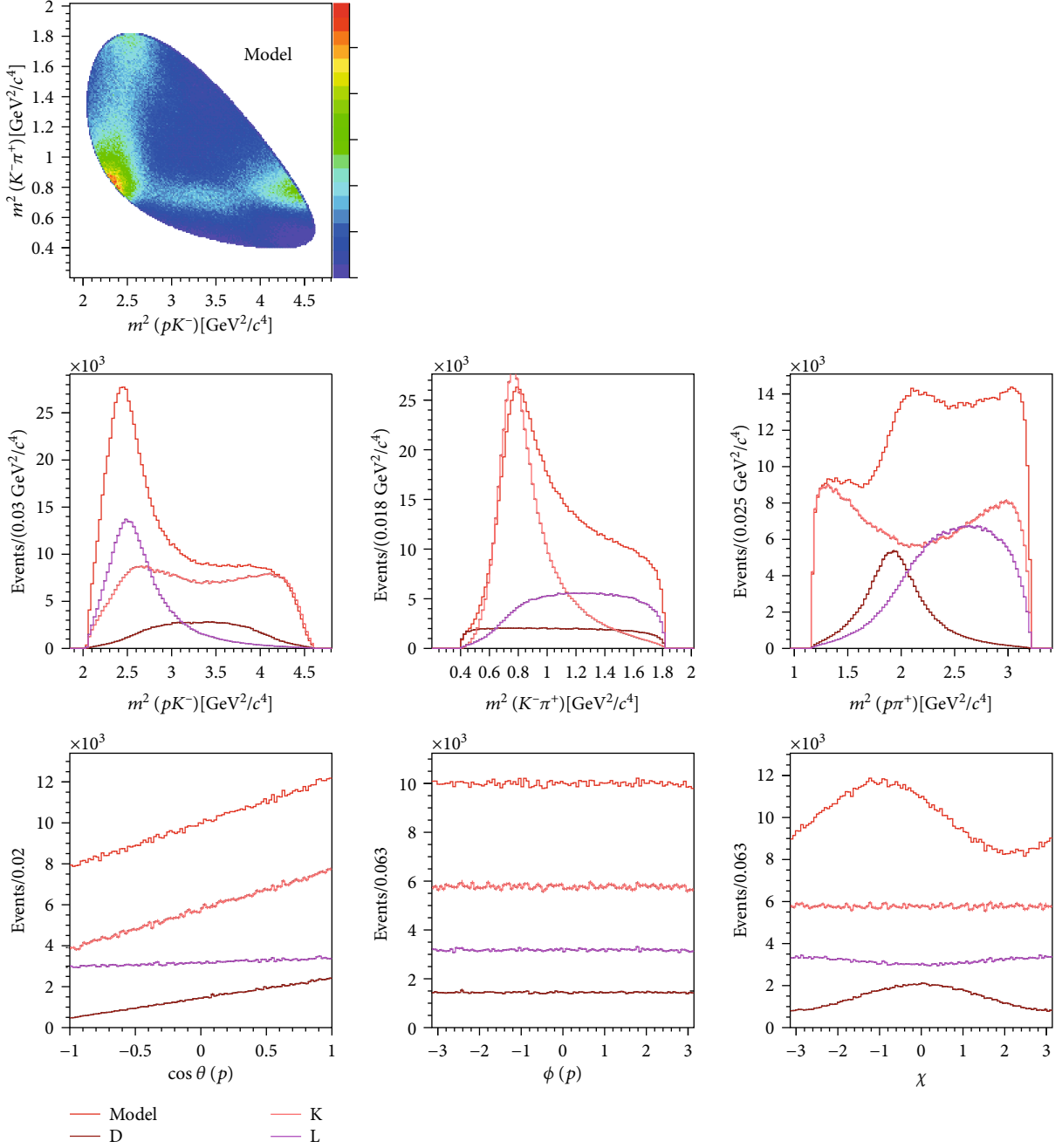
FIGURE 3: $\Lambda_c^+ \longrightarrow pK^-\pi^+$ toy amplitude model projections $P_z = 1$, generated using one million Monte Carlo events.

presented in Section 1, ranging from New Physics searches to low-energy QCD studies. In particular, the $\Lambda_c^+ \longrightarrow pK^-\pi^+$ decay can be used as an absolute polarimeter for the Λ_c^+ baryon.

Appendix

A. Explicit d-Matrices Expressions

Here, we report the explicit d-matrices expressions employed throughout the article.

The Wigner d-matrix for spin 1/2 is

$$d_{m',m}^{1/2}(\theta) = \begin{pmatrix} \cos\dfrac{\theta}{2} & -\sin\dfrac{\theta}{2} \\ \sin\dfrac{\theta}{2} & \cos\dfrac{\theta}{2} \end{pmatrix}. \tag{A.1}$$

The Wigner d-matrix elements $m', m = \pm 1/2$ for semi-integer spin s can be written in the form:

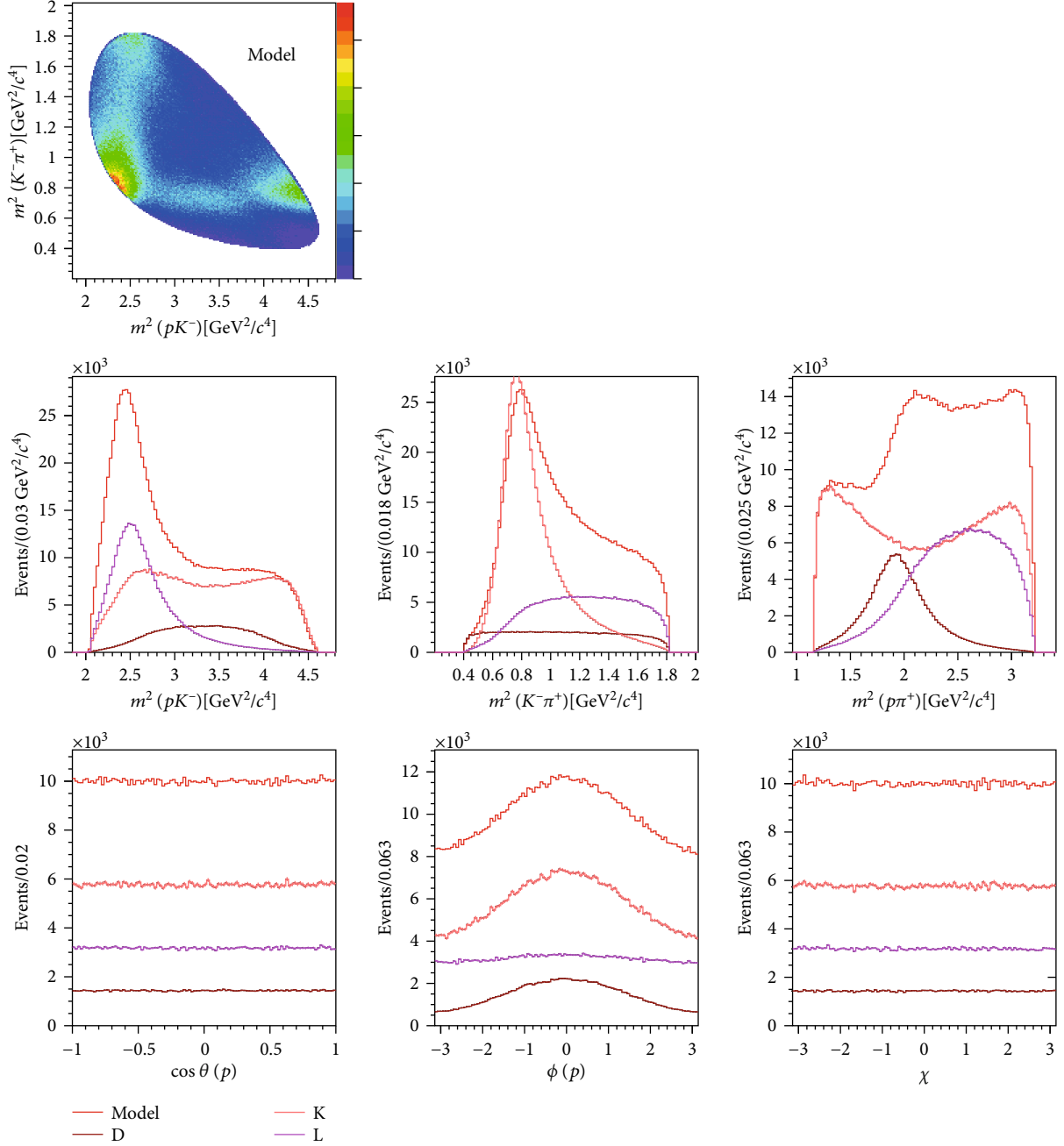$$d_{m',m}^{S}(\theta) = f(S,\theta) d_{m',m}^{1/2}(\theta). \tag{A.2}$$

FIGURE 4: $\Lambda_c^+ \longrightarrow pK^-\pi^+$ toy amplitude model projections for $P_x = 1$, generated using one million Monte Carlo events.

For instance,

$$f(1/2, ,\theta) = 1,$$

$$f(3/2, \theta) = \frac{1}{2}(3\cos\theta - 1).$$

(A.3)

B. Projections of the $\Lambda_c^+ \to pK^-\pi^+$ Toy Amplitude Model

We consider the projections of the $\Lambda_c^+ \longrightarrow pK^-\pi^+$ toy amplitude model described in Section 6 for different Λ_c^+ polarisation components: P_z in Figure 3, P_x in Figure 4, and P_y in Figure 5.

The orientation angle projections follow the dependencies predicted in Section 5.2: a P_z component produces a linear $\cos\theta_p$ and a sinusoidal χ dependence, while a $P_x(P_y)$ component gives rise to a cosine (minus sine) dependence in ϕ_p. Invariant mass distributions are independent on the polarisation for rotational invariance as explained in Section 2.2.

Data Availability

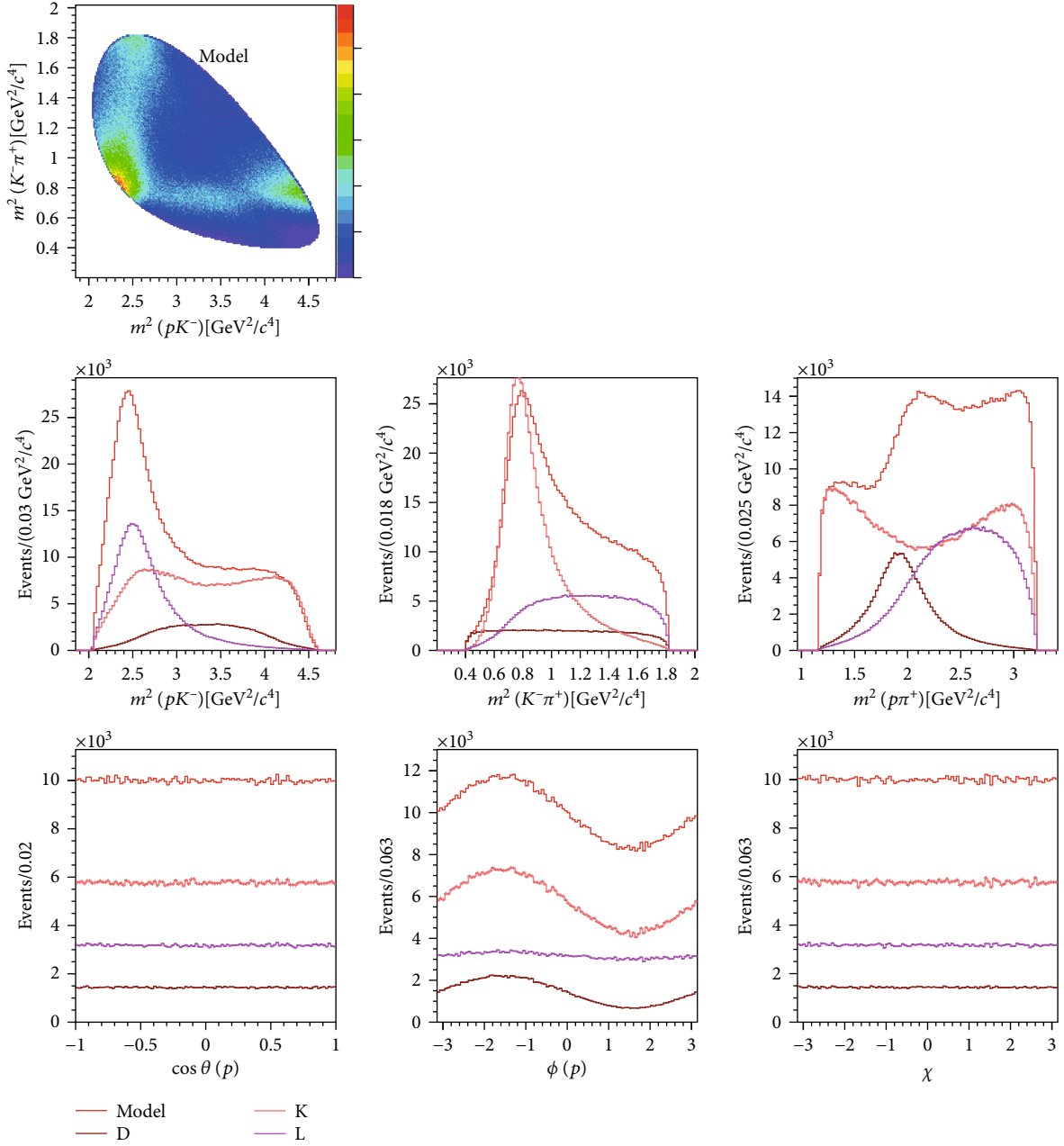The data used to support the findings of this study are included within the article.

FIGURE 5: $\Lambda_c^+ \longrightarrow pK^-\pi^+$ toy amplitude model projections for $P_y = 1$, generated using one million Monte Carlo events.

Conflicts of Interest

The author declares that there are no conflicts of interest.

Acknowledgments

References

[1] D. Marangotto, *Amplitude analysis and polarisation measurement of the Λ_c^+ baryon in $pK^-\pi^+$ final state for electromagnetic dipole moment experiment, [Ph.D. thesis]*, Universit degli studi di Milano, 2020, https://cds.cern.ch/record/2713231.

[2] R. Dutta, "$\Lambda_b \longrightarrow (\Lambda_c, p)\tau\nu$ decays within standard model and beyond," *Physical Review D*, vol. 93, no. 5, article 054003, 2016.

[3] S. Shivashankara, W. Wu, and A. Datta, "$\Lambda_b \longrightarrow \Lambda_c \tau \bar{\nu}_\tau$ decay in the standard model and with new physics," *Physical Review D*, vol. 91, no. 11, article 115003, 2015.

[4] X.-Q. Li, Y.-D. Yang, and X. Zhang, "$\Lambda_b \longrightarrow \Lambda_c \tau \bar{\nu}_\tau$ decay in scalar and vector leptoquark scenarios," *Journal of High Energy Physics*, vol. 2017, no. 2, article 68, 2017.

[5] A. Datta, S. Kamali, S. Meinel, and A. Rashed, "Phenomenology of $\Lambda_b \longrightarrow \Lambda_c \tau \bar{\nu}_\tau$ using lattice QCD calculations," *Journal of High Energy Physics*, vol. 2017, no. 8, 2017.

[6] E. Di Salvo, F. Fontanelli, and Z. J. Ajaltouni, "Detailed study of the decay $\Lambda_b \longrightarrow \Lambda_c \tau \bar{\nu}_\tau$," 2018, https://arxiv.org/abs/1804.05592.

[7] A. Ray, S. Sahoo, and R. Mohanta, "Probing new physics in semileptonic Λ_b decays," *Physical Review D*, vol. 99, no. 1, article 015015, 2019.

[8] P. Böer, A. Kokulu, J.-N. Toelstede, and D. van Dyk, "Angular Analysis of $\Lambda_b(\longrightarrow \Lambda \pi)\ell\bar{\nu}$," *Journal of High Energy Physics*, vol. 2019, article 82, 2019.

[9] N. Pefinalva, E. HernÆndez, and J. Nieves, "Further tests of lepton avour universality from the charged lepton energy distribution in $b \longrightarrow c$ semileptonic decays: The case of $\Lambda_b \longrightarrow \Lambda_c \ell \bar{\nu}_\ell$," https://arxiv.org/abs/1908.02328.

[10] T. Mannel and G. A. Schuler, "Semileptonic decays of bottom baryons at LEP," *Physics Letters B*, vol. 279, p. 194, 1992.

[11] A. F. Falk and M. E. Peskin, "Production, decay, and polarization of excited heavy hadrons," *Physical Review D*, vol. 49, no. 7, pp. 3320–3332, 1994.

[12] M. Galanti, A. Giammanco, Y. Grossman, Y. Kats, E. Stamou, and J. Zupan, "Heavy baryons as polarimeters at colliders," *Journal of High Energy Physics*, vol. 2015, no. 11, 2015.

[13] Particle Data Group, "Review of particle physics," *Physical Review D*, vol. 98, article 030001, 2018.

[14] F. J. Botella, L. M. Garcia Martin, D. Marangotto et al., "On the search for the electric dipole moment of strange and charm baryons at LHC," *The European Physical Journal C*, vol. 77, no. 3, article 181, 2017.

[15] E. Bagli, L. Bandiera, G. Cavoto et al., "Electromagnetic dipole moments of charged baryons with bent crystals at the LHC," *The European Physical Journal C*, vol. 77, no. 12, article 828, 2017.

[16] E. M. Aitala, S. Amato, J. C. Anjos et al., "Multidimensional resonance analysis of $\Lambda c^+ \longrightarrow pK^- \pi^+$," *Physics Letters B*, vol. 471, no. 4, pp. 449–459, 2000.

[17] J. G. Korner and M. Kramer, "Exclusive nonleptonic charm baryon decays," *Zeitschrift für Physik*, vol. 55, p. 659, 1992.

[18] P. Bialas, J. G. Körner, M. Krämer, and K. Zalewski, "Joint angular decay distributions in exclusive weak decays of heavy mesons and baryons," *Zeitschrift für Physik C Particles and Fields*, vol. 57, no. 1, pp. 115–134, 1993.

[19] B. König, J. G. Körner, and M. Krämer, "On the determination of the $b \longrightarrow c$ handedness using nonleptonic Λ_c decays," *Physical Review D*, vol. 49, pp. 2363–2368, 1994.

[20] B. König, J. G. Körner, M. Krämer, and P. Kroll, "In nite momentum frame calculation of semileptonic heavy $\Lambda_b \longrightarrow \Lambda_c$ transitions including HQET improvements," *Physical Review D*, vol. 56, pp. 4282–4294, 1997.

[21] J.-Y. Cen, C.-Q. Geng, C.-W. Liu, and T.-H. Tsai, "Up-down asymmetries of charmed baryon three-body decays," *The European Physical Journal C*, vol. 79, no. 11, 2019.

[22] E. Leader, "Spin in particle physics," in *Cambridge Monographs on Particle Physics Nuclear Physics and Cosmology*, vol. 15, Cambridge University Press, 2011.

[23] D. Marangotto, "Helicity formalism revisited for polarised particle decays," https://arxiv.org/abs/1911.10025.

[24] M. Jacob and G. C. Wick, "On the general theory of collisions for particles with spin," *Annals of Physics*, vol. 7, no. 4, pp. 404–428, 1959.

[25] J. D. Richman, "An experimenter's guide to the helicity formalism," CALT-68-1148.

[26] M. Mikhasenko, M. Albaladejo, Ł. Bibrzycki et al., "Dalitz-plot decomposition for three-body decays," *Physical Review D*, vol. 101, no. 3, article 034033, 2020.

[27] E. Gourgoulhon, *Special Relativity in General Frames*, Springer, 2013.

[28] G. Breit and E. Wigner, "Capture of slow neutrons," *Physical Review*, vol. 49, no. 7, pp. 519–531, 1936.

[29] "TensorFlowAnalysis: A collection of useful functions and example scripts for performing amplitude fits using TensorFlow," https://gitlab.cern.ch/poluekt/TensorFlowAnalysis.

[30] M. Abadi, A. Agarwal, P. Barham et al., *TensorFlow: Large-Scale Machine Learning on Heterogeneous Systems*, 2015, https://www.tensorflow.org.

[31] F. James and M. Roos, "Minuit: a system for function minimization and analysis of the parameter errors and correlations," *Computer Physics Communications*, vol. 10, no. 6, pp. 343–367, 1975.

[32] R. Brun and F. Rademakers, "ROOT: an object oriented data analysis framework," *Nuclear Instruments and Methods in Physics Research A*, vol. 389, pp. 81–86, 1997.